Nonlinear dynamics of a solid particle in an acoustically excited viscoelastic fluid. I. Acoustic streaming

Alexander A. Doinikov ⦾, Jonas Fankhauser ⦾, and Jürg Dual
Department of Mechanical and Process Engineering, Institute for Mechanical Systems (IMES),
Swiss Federal Institute of Technology (ETH Zurich), Tannenstrasse 3, 8092 Zurich, Switzerland

An analytical theory is developed for acoustic streaming induced by an axisymmetric acoustic wave field around an isotropic solid spherical particle in a compressible viscoelastic fluid. The particle is assumed to undergo pulsation, translation, and shape deformations of all orders. The fluid motion is described by the compressible Oldroyd-B model. No restrictions are imposed on the particle size with respect to the acoustic wavelength and the viscous penetration depth. The obtained analytical solutions are used in numerical simulations. It is shown that in the general case, the streaming velocity magnitude decreases with increasing polymer viscosity. Increasing relaxation time (elasticity) of the polymer solution leads to increasing streaming velocity magnitude as long as the relaxation time remains relatively small. It is also observed that the variation of the polymer viscosity and the relaxation time can change the pattern of streamlines.

I. INTRODUCTION

Many microfluidic applications involve handling fluids with a complex microstructure, such as polymeric solutions, blood, or protein solutions. The flow of such fluids is characterized by non-Newtonian behavior and, in particular, viscoelasticity [1]. Microchannel devices designed to focus, concentrate, or separate particles suspended in viscoelastic fluids are becoming common [2–4]. Recent progress in the field is reviewed in Ref. [5]. It is well known that the elastic part of the fluid response will increase, for example, the thickness of the boundary layer for the first-order solutions and therefore also influences the higher-order results of acoustic streaming and acoustic radiation force. The viscoelastic behavior makes more complicated the modeling of processes that occur in microfluidic systems. One of these processes, rarely explored, is acoustic streaming that is generated around a particle suspended in an acoustically excited viscoelastic fluid. This fact has inspired the present study.

Acoustic streaming is a well-known phenomenon, which has been the subject of much research [6–12]. However, all available theoretical studies are devoted to Newtonian fluids. Our study is an attempt to obtain analytical solutions for acoustic streaming that develops around an isotropic solid particle in a viscoelastic fluid. Our derivation is performed in a maximally general form. We assume that the particle undergoes oscillation modes of all orders (pulsation, translation, shape deformations). Allowing for shape modes is important because acoustic streaming is known to be produced by nonspherical oscillations. A correct calculation of the acoustic radiation force also requires taking account of higher oscillation modes.

We do not impose any restrictions on the particle size with respect to the acoustic wavelength and the viscous penetration depth. In contrast to the universally accepted approach to

neglect the fluid compressibility when solving the equations of acoustic streaming (Nyborg's approximation [6]), we take it into account. It is known that the fluid compressibility can be ignored when acoustic microstreaming is calculated. However, the calculation of the primary acoustic radiation force is impossible if the fluid compressibility is ignored. Since the general theory developed in this paper (Part I) is then used in Part II [13] to calculate the radiation force, we take account of the fluid compressibility.

II. THEORY

A. Problem formulation

We consider a solid particle immersed in a viscoelastic fluid, which is excited by an axisymmetric acoustic wave; see Fig. 1. We assume that the particle is spherical at rest. In response to acoustic excitation, the particle undergoes pulsation, translation, and shape deformations of all orders.

Assuming that the elastic deformations experienced by the particle are small, we describe the motion of the solid inside the particle by the Navier equation [14],

$$\frac{\partial^2 \boldsymbol{u}}{\partial t^2} = c_2^2 \nabla^2 \boldsymbol{u} + \left(c_1^2 - c_2^2\right) \nabla (\nabla \cdot \boldsymbol{u}), \tag{1}$$

where $\boldsymbol{u}$ is the displacement vector, c_1 is the primary wave speed, calculated by

$$c_1 = \sqrt{\frac{E(1-\nu)}{\rho_s(1+\nu)(1-2\nu)}}, \tag{2}$$

and c_2 is the secondary wave speed, calculated by

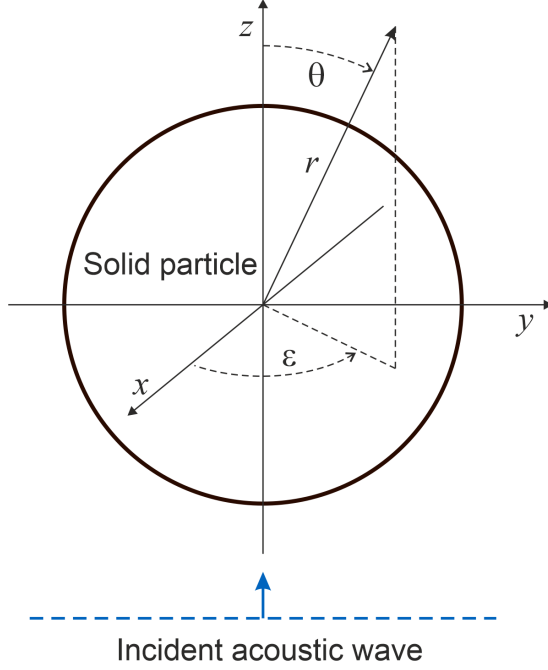$$c_2 = \sqrt{\frac{E}{2\rho_s(1+\nu)}}. \tag{3}$$

FIG. 1. Geometry of the system under study. A solid particle is immersed in a viscoelastic fluid subject to an axisymmetric acoustic wave.

Here, ρ_s is the solid density, E is Young's modulus, and ν is Poisson's ratio.

The motion of the fluid surrounding the particle is described by the continuity equation and the momentum equation [15],

$$\frac{\partial \rho}{\partial t} + \boldsymbol{\nabla} \cdot (\rho \boldsymbol{v}) = 0, \tag{4}$$

$$\rho \left(\frac{\partial \boldsymbol{v}}{\partial t} + \boldsymbol{v} \cdot \boldsymbol{\nabla} \boldsymbol{v} \right) = \boldsymbol{\nabla} \cdot \boldsymbol{\sigma}, \tag{5}$$

where ρ is the fluid density, $\boldsymbol{v}$ is the fluid velocity, $\boldsymbol{\sigma}$ is the stress tensor with components σ_{ik}, and the product $\boldsymbol{\nabla} \cdot \boldsymbol{\sigma}$ means $\nabla_k \sigma_{ik}$ with summation over repeated indices.

The stress tensor $\boldsymbol{\sigma}$ is specified by the compressible Oldroyd-B model [16],

$$\boldsymbol{\sigma} = -p\boldsymbol{I} + \eta_f \left[\boldsymbol{\nabla} \boldsymbol{v} + (\boldsymbol{\nabla} \boldsymbol{v})^T - \tfrac{2}{3}(\boldsymbol{\nabla} \cdot \boldsymbol{v})\boldsymbol{I} \right] + \zeta_f(\boldsymbol{\nabla} \cdot \boldsymbol{v})\boldsymbol{I} + \boldsymbol{\tau}, \tag{6}$$

where p is the hydrodynamic pressure; $\boldsymbol{I}$ is the identity tensor; the superscript T denotes the transpose of a tensor; η_f, ζ_f are the fluid (solvent) shear and volume viscosities; and $\boldsymbol{\tau}$ is a second-rank tensor that describes the polymer effect and is defined by

$$\boldsymbol{\tau} + \lambda_M \left[\frac{\partial \boldsymbol{\tau}}{\partial t} + \boldsymbol{v} \cdot \boldsymbol{\nabla} \boldsymbol{\tau} - \boldsymbol{\tau} \cdot \boldsymbol{\nabla} \boldsymbol{v} - (\boldsymbol{\nabla} \boldsymbol{v})^T \cdot \boldsymbol{\tau} \right]$$
$$= \eta_p \left[\boldsymbol{\nabla} \boldsymbol{v} + (\boldsymbol{\nabla} \boldsymbol{v})^T - \frac{2}{3}(\boldsymbol{\nabla} \cdot \boldsymbol{v})\boldsymbol{I} \right] + \zeta_p(\boldsymbol{\nabla} \cdot \boldsymbol{v})\boldsymbol{I}, \tag{7}$$

where λ_M is the Maxwell relaxation time and η_p, ζ_p are the polymer contributions to the total shear and volume viscosities, respectively. It should be mentioned that the Oldroyd-B model is often written in a different mathematical form, where

parameters called the total viscosity $\eta_0 = \eta_f + \eta_p$ and the retardation time $\lambda_r = (\eta_f/\eta_0)\lambda_M$ are used [16].

It should be noted that, unfortunately, there is no single model that describes all viscoelastic fluids similar to the Navier-Stokes equations for Newtonian flows. The Oldroyd-B model is considered in the literature as one of the most popular models, which adequately describes a wide range of polymer solutions and biological fluids. At the same time, it is one of the simplest rheological models for fluids that have some elastic effects and a viscous fluid as a limiting case. Therefore, we have chosen this model. Its mathematical derivation and detailed analysis are given in Ref. [16]. The Oldroyd-B model can be regarded as an extension of the upper-convected Maxwell model, which results in a combination of the viscoelastic stress and the Newtonian stress [16], or as an extension of the linear Jeffreys model to nonlinear flows [17]. All these models are used to study oscillatory flows in viscoelastic fluids. Solutions to classical problems, such as wave propagation in viscoelastic fluids and the behavior of Stokes layers, can be found in Refs. [18–20]. Theoretical and numerical investigations of bubble oscillations in viscoelastic fluids have been performed by Shima *et al.* [21] using the Oldroyd-B model and more recently by Allen and Roy [22] employing the Jeffreys model. Hintermüller *et al.* [23] used the upper-convected Maxwell model and a perturbation approach in order to model acoustic streaming in a simple rectangular geometry.

In the next subsections, we first solve Eq. (1) to obtain deformations inside the particle. We then linearize Eqs. (4)–(7) and solve them to obtain the first-order scattered velocity field in the fluid. In the course of calculating the first-order solutions, we use the boundary condition that the velocity and the stress are continuous through the surface of the particle. We also use the condition that the scattered field vanishes at infinity. Then we write down Eqs. (4)–(7) up to second-order terms and average them over time. As a result, we obtain equations of acoustic streaming. Their solution is the ultimate goal of our derivation. In the course of solving the equations of acoustic streaming, we use the boundary condition of adhesion of the fluid to the surface of the solid particle and the condition that the streaming vanishes at infinity.

B. Solutions inside the particle

The displacement vector $\boldsymbol{u}$ is represented by the Helmholtz decomposition:

$$\boldsymbol{u} = \boldsymbol{\nabla} \varphi_s + \boldsymbol{\nabla} \times \boldsymbol{\psi}_s. \tag{8}$$

Substitution of Eq. (8) into Eq. (1) yields

$$\nabla^2 \varphi_s + k_1^2 \varphi_s = 0, \tag{9}$$

$$\nabla^2 \boldsymbol{\psi}_s + k_2^2 \boldsymbol{\psi}_s = 0, \tag{10}$$

where $k_1 = \omega/c_1$ and $k_2 = \omega/c_2$ are the wave numbers of the primary and secondary waves, respectively.

In view of the axial symmetry of the problem, a solution to Eq. (9) is given by

$$\varphi_s(r, \theta, t) = e^{-i\omega t} \sum_{n=0}^{\infty} \widehat{a}_n j_n(k_1 r) P_n(\mu), \tag{11}$$

while a solution to Eq. (10) is given by

$$\boldsymbol{\psi}_s = \psi_s \boldsymbol{e}_\varepsilon, \tag{12}$$

where $\boldsymbol{e}_\varepsilon$ is the unit azimuth vector and ψ_s is calculated by

$$\psi_s(r, \theta, t) = e^{-i\omega t} \sum_{n=1}^{\infty} \widehat{b}_n j_n(k_2 r) P_n^1(\mu). \tag{13}$$

Here, j_n is the spherical Bessel function; P_n is the Legendre polynomial of degree n; $\mu = \cos\theta$; P_n^1 is the associated Legendre polynomial of the first order and degree n; and $\widehat{a}_n, \widehat{b}_n$ are constant coefficients, which are calculated in Appendix A.

The radial and tangential components of $\boldsymbol{u}$ are calculated by

$$u_r = e^{-i\omega t} \sum_{n=0}^{\infty} \left[k_1 \widehat{a}_n j_n'(k_1 r) - n(n+1)\widehat{b}_n \frac{j_n(k_2 r)}{r} \right] P_n(\mu), \tag{14}$$

$$u_\theta = \frac{e^{-i\omega t}}{r} \sum_{n=1}^{\infty} \{\widehat{a}_n j_n(k_1 r) - \widehat{b}_n [j_n(k_2 r) + k_2 r j_n'(k_2 r)]\} P_n^1(\mu), \tag{15}$$

where the prime denotes the derivative with respect to an argument in brackets.

C. First-order solutions in the fluid

Linearization of Eqs. (4)–(7) yields

$$\frac{\partial \rho^{(1)}}{\partial t} + \rho_0 \nabla \cdot \boldsymbol{v}^{(1)} = 0, \tag{16}$$

$$\rho_0 \frac{\partial \boldsymbol{v}^{(1)}}{\partial t} = -\nabla p^{(1)} + \eta_f \nabla^2 \boldsymbol{v}^{(1)}$$
$$+ \left(\zeta_f + \frac{\eta_f}{3}\right) \nabla(\nabla \cdot \boldsymbol{v}^{(1)}) + \nabla \cdot \boldsymbol{\tau}^{(1)}, \tag{17}$$

$$\boldsymbol{\tau}^{(1)} + \lambda_M \frac{\partial \boldsymbol{\tau}^{(1)}}{\partial t} = \eta_p \left[\nabla \boldsymbol{v}^{(1)} + (\nabla \boldsymbol{v}^{(1)})^T - \frac{2}{3}(\nabla \cdot \boldsymbol{v}^{(1)})\boldsymbol{I} \right]$$
$$+ \zeta_p (\nabla \cdot \boldsymbol{v}^{(1)})\boldsymbol{I}, \tag{18}$$

where ρ_0 is the equilibrium fluid density.

Providing the time dependence is $\exp(-i\omega t)$, Eqs. (17) and (18) are transformed to

$$\rho_0 \frac{\partial \boldsymbol{v}^{(1)}}{\partial t} = -\nabla p^{(1)} + \eta_c \nabla^2 \boldsymbol{v}^{(1)} + \left(\zeta_c + \frac{\eta_c}{3}\right) \nabla(\nabla \cdot \boldsymbol{v}^{(1)}), \tag{19}$$

where η_c and ζ_c are complex viscosities defined by

$$\eta_c = \eta_f + \frac{\eta_p}{1 - i\omega \lambda_M}, \quad \zeta_c = \zeta_f + \frac{\zeta_p}{1 - i\omega \lambda_M}. \tag{20}$$

Equations (16)–(20) are supplemented with the state equation,

$$p^{(1)} - p_0 = c^2(\rho^{(1)} - \rho_0), \tag{21}$$

where p_0 is the equilibrium pressure in the fluid and c is the speed of sound in the fluid.

Thus, the first-order fluid motion is described by Eqs. (16), (19), and (21).

The first-order fluid velocity is represented by

$$\boldsymbol{v}^{(1)} = \nabla \varphi^{(1)} + \nabla \times \boldsymbol{\psi}^{(1)}. \tag{22}$$

With Eq. (22), Eqs. (16), (19), and (21) are transformed to

$$\nabla^2 \varphi^{(1)} + k_f^2 \varphi^{(1)} = 0, \tag{23}$$

$$\nabla^2 \boldsymbol{\psi}^{(1)} + k_v^2 \boldsymbol{\psi}^{(1)} = 0, \tag{24}$$

where the wave numbers k_f and k_v are given by

$$k_f = \frac{\omega}{c} \left[1 - \frac{i\omega}{\rho_0 c^2}\left(\zeta_c + \frac{4\eta_c}{3}\right) \right]^{-\frac{1}{2}}, \quad k_v = (1 + i)\sqrt{\frac{\rho_0 \omega}{2\eta_c}}. \tag{25}$$

By analogy with a viscous fluid, we can introduce a viscous boundary layer thickness δ and a viscous wavelength λ_v in a viscoelastic fluid. Since the viscosity η_c is now complex valued, these quantities are defined as $\delta = 1/\text{Im}\{k_v\}$ and $\lambda_v = 2\pi/\text{Re}\{k_v\}$. Note that in a viscous fluid, $\lambda_v/\delta = 2\pi$. In a viscoelastic fluid, this is no longer the case. See Sec. III for more information.

In our case, the first-order fluid velocity is a sum of the velocity of the driving acoustic wave, $\boldsymbol{v}_{ac}$, and the velocity of the scattered wave produced by the particle, $\boldsymbol{v}_{sc}^{(1)}$,

$$\boldsymbol{v}^{(1)} = \boldsymbol{v}_{ac} + \boldsymbol{v}_{sc}^{(1)}. \tag{26}$$

We assume that the driving acoustic wave is irrotational and hence its velocity can be represented by

$$\boldsymbol{v}_{ac} = \nabla \varphi_{ac}, \tag{27}$$

where, in view of axial symmetry, φ_{ac} is calculated by [24]

$$\varphi_{ac}(r, \theta, t) = e^{-i\omega t} \sum_{n=0}^{\infty} A_n j_n(k_f r) P_n(\mu). \tag{28}$$

For a plane traveling wave, $A_n = A(2n + 1)i^n$, and for a plane standing wave, $A_n = (A/2)(2n + 1)i^n[e^{ik_f d} + (-1)^n e^{-ik_f d}]$, where A is the amplitude of the velocity potential and d is the distance between the equilibrium center of the particle and the nearest velocity node of the standing wave.

According to Eq. (22), the scattered velocity is written as

$$\boldsymbol{v}_{sc}^{(1)} = \nabla \varphi_{sc}^{(1)} + \nabla \times \boldsymbol{\psi}_{sc}^{(1)}, \tag{29}$$

where, as follows from Eqs. (23) and (24), in view of axial symmetry, $\varphi_{sc}^{(1)}$ is calculated by

$$\varphi_{sc}^{(1)}(r, \theta, t) = e^{-i\omega t} \sum_{n=0}^{\infty} a_n h_n^{(1)}(k_f r) P_n(\mu), \tag{30}$$

while $\boldsymbol{\psi}_{sc}^{(1)}$ is given by

$$\boldsymbol{\psi}_{sc}^{(1)} = \psi_{sc}^{(1)} \boldsymbol{e}_\varepsilon, \tag{31}$$

where $\psi_{sc}^{(1)}$ is calculated by

$$\psi_{sc}^{(1)}(r, \theta, t) = e^{-i\omega t} \sum_{n=1}^{\infty} b_n h_n^{(1)}(k_v r) P_n^1(\mu). \tag{32}$$

Here, $h_n^{(1)}$ is the spherical Hankel function of the first kind and a_n, b_n are constant coefficients, commonly called linear scattering coefficients, which are calculated in Appendix A.
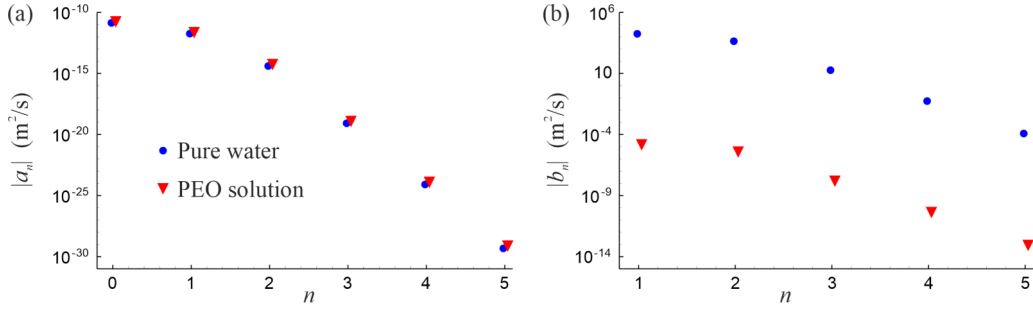
FIG. 2. The magnitude of the linear scattering coefficients at increasing values of the mode number n in pure water and in a water solution of polyethylene oxide (PEO) with $\eta_p = 0.009$ Pa s and $\lambda_M = 10^{-6}$ s. The driving is a 100 kHz, 10 kPa plane traveling wave. The particle radius is $R_0 = 50$ μm.

It follows from Eq. (22) that the radial and tangential components of the total first-order fluid velocity are calculated by

$$v_r^{(1)} = \frac{\partial \varphi^{(1)}}{\partial r} + \frac{1}{r \sin \theta} \frac{\partial}{\partial \theta} \left(\sin \theta \, \psi_{sc}^{(1)} \right)$$

$$= e^{-i\omega t} \sum_{n=0}^{\infty} V_{rn}(r) P_n(\mu), \tag{33}$$

$$v_\theta^{(1)} = \frac{1}{r} \frac{\partial \varphi^{(1)}}{\partial \theta} - \frac{1}{r} \frac{\partial}{\partial r} \left(r \psi_{sc}^{(1)} \right) = e^{-i\omega t} \sum_{n=1}^{\infty} V_{\theta n}(r) P_n^1(\mu), \tag{34}$$

where

$$V_{rn}(r) = A_n k_f j_n'(k_f r) + a_n k_f h_n^{(1)'}(k_f r) - n(n+1) b_n \frac{h_n^{(1)}(k_v r)}{r}, \tag{35}$$

$$V_{\theta n}(r) = \frac{1}{r} \Big\{ A_n j_n(k_f r) + a_n h_n^{(1)}(k_f r) - b_n \big[h_n^{(1)}(k_v r) + k_v r h_n^{(1)'}(k_v r) \big] \Big\}. \tag{36}$$

Note that Eqs. (33) and (34) include oscillation modes of all orders.

D. Acoustic streaming

Taking Eqs. (4)–(7) up to second-order terms and averaging over time, one obtains

$$\nabla \cdot \langle \boldsymbol{v}^{(2)} \rangle = -\frac{1}{\rho_0} \nabla \cdot \langle \rho^{(1)} \boldsymbol{v}^{(1)} \rangle, \tag{37}$$

$$(\eta_f + \eta_p) \nabla^2 \langle \boldsymbol{v}^{(2)} \rangle + \left(\zeta_f + \zeta_p + \frac{\eta_f + \eta_p}{3} \right) \nabla (\nabla \cdot \langle \boldsymbol{v}^{(2)} \rangle) - \nabla \langle p^{(2)} \rangle$$

$$= \rho_0 \langle \boldsymbol{v}^{(1)} \nabla \cdot \boldsymbol{v}^{(1)} + \boldsymbol{v}^{(1)} \cdot \nabla \boldsymbol{v}^{(1)} \rangle + \lambda_M \langle \nabla \cdot \mathbf{T} \rangle, \tag{38}$$

where $\langle \cdots \rangle$ means the time average and $\mathbf{T}$ is a second-rank tensor that is defined by

$$\mathbf{T} = \boldsymbol{v}^{(1)} \cdot \nabla \boldsymbol{\tau}^{(1)} - \boldsymbol{\tau}^{(1)} \cdot \nabla \boldsymbol{v}^{(1)} - (\nabla \boldsymbol{v}^{(1)})^T \cdot \boldsymbol{\tau}^{(1)}, \tag{39}$$

where, as follows from Eq. (18), $\boldsymbol{\tau}^{(1)}$ is calculated by

$$\boldsymbol{\tau}^{(1)} = \frac{\eta_p}{1 - i\omega\lambda_M} \left[\nabla \boldsymbol{v}^{(1)} + (\nabla \boldsymbol{v}^{(1)})^T - \frac{2}{3} (\nabla \cdot \boldsymbol{v}^{(1)}) \boldsymbol{I} \right]$$

$$+ \frac{\zeta_p}{1 - i\omega\lambda_M} (\nabla \cdot \boldsymbol{v}^{(1)}) \boldsymbol{I}. \tag{40}$$

Equations (37) and (38) describe acoustic streaming and their solution, $\langle \boldsymbol{v}^{(2)} \rangle$, is the Eulerian velocity of the acoustic streaming.
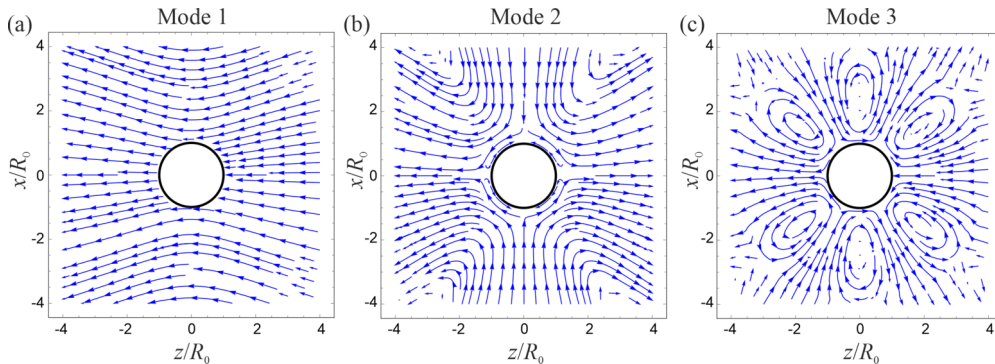

FIG. 3. Streamline patterns for modes with $n = 1$, 2, 3. The driving is a 100 kHz, 10 kPa plane traveling wave. The fluid is a water solution of PEO with $\eta_p = 0.009$ Pa s and $\lambda_M = 10^{-6}$ s. The particle radius is $R_0 = 50$ μm.
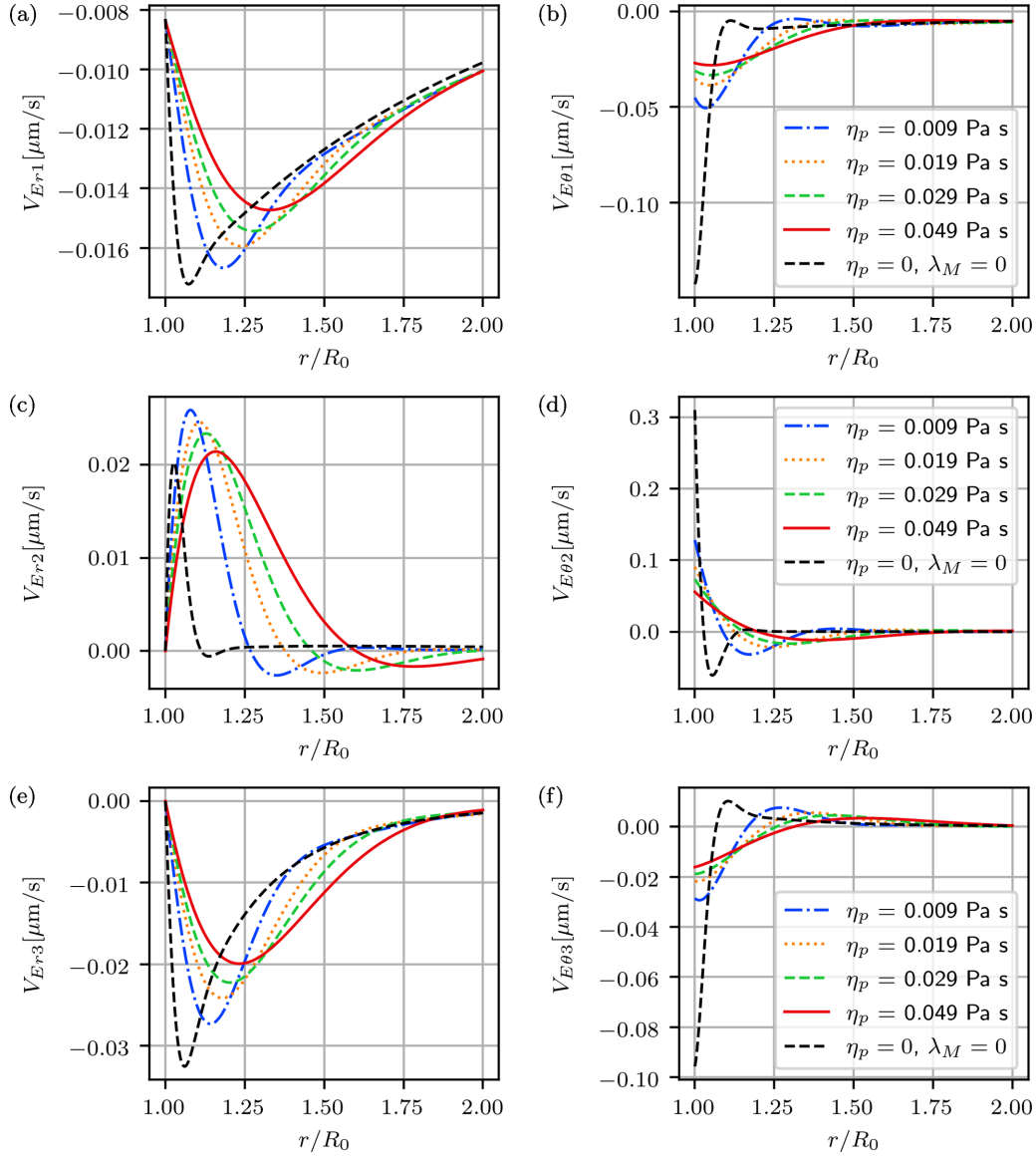
FIG. 4. The r dependence of the components of the Eulerian streaming velocity at different values of η_p for modes with $n = 1, \ 2, \ 3$. The other parameters are as in Fig. 3. The values of η_p have been chosen so as to get round numbers for the total shear viscosity.

The streaming velocity $\langle \boldsymbol{v}^{(2)} \rangle$ is sought as

$$\langle \boldsymbol{v}^{(2)} \rangle = \nabla \Phi + \nabla \times \boldsymbol{\Psi}, \tag{41}$$

where, in view of axial symmetry, $\Phi = \Phi(r, \theta)$ and $\boldsymbol{\Psi} = \Psi(r, \theta) \boldsymbol{e}_\varepsilon$.

Substitution of Eq. (41) into Eq. (37) yields

$$\nabla^2 \Phi = -\frac{1}{\rho_0} \nabla \cdot \langle \rho^{(1)} \boldsymbol{v}^{(1)} \rangle. \tag{42}$$

With the help of Eqs. (16) and (23), Eq. (42) is transformed to

$$\nabla^2 \Phi = -\frac{1}{\omega} \nabla \cdot \langle i k_f^2 \varphi^{(1)} \boldsymbol{v}^{(1)} \rangle, \tag{43}$$

where $\varphi^{(1)} = \varphi_{\mathrm{ac}} + \varphi_{\mathrm{sc}}^{(1)}$.

Substituting Eq. (41) into Eq. (38) and calculating the curl of the resulting equation [6,25], one obtains

$$\nabla^4 \boldsymbol{\Psi} = -\frac{\rho_0}{\eta_f + \eta_p} \nabla \times \langle \boldsymbol{v}^{(1)} \nabla \cdot \boldsymbol{v}^{(1)} + \boldsymbol{v}^{(1)} \cdot \nabla \boldsymbol{v}^{(1)} \rangle$$
$$- \frac{\lambda_M}{\eta_f + \eta_p} \nabla \times \langle \nabla \cdot \mathbf{T} \rangle. \tag{44}$$

Equations (43) and (44) are solved in Appendixes B and C, respectively. The solutions are given by

$$\Phi = \sum_{l=0}^{\infty} \Phi_l(r) P_l(\mu), \tag{45}$$

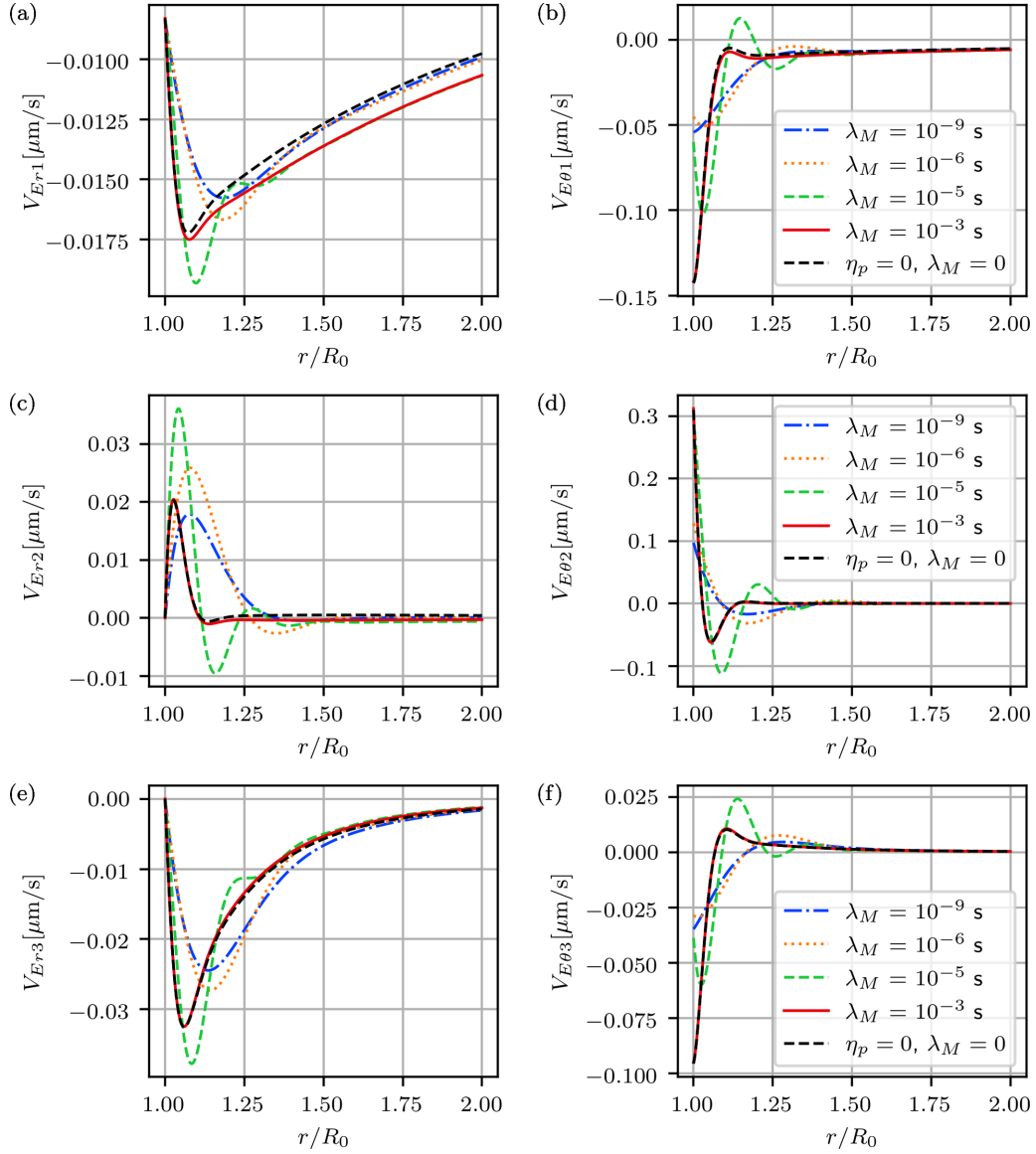$$\boldsymbol{\Psi} = \boldsymbol{e}_\varepsilon \sum_{l=1}^{\infty} \Psi_l(r) P_l^1(\mu), \tag{46}$$

FIG. 5. The r dependence of the components of the Eulerian streaming velocity at different values of λ_M for modes with $n = 1, 2, 3$. The other parameters are as in Fig. 3.

where $\Phi_l(r)$ and $\Psi_l(r)$ are calculated by Eqs. (B12) and (C18), respectively.

Substituting Eqs. (45) and (46) into Eq. (41) gives the components of the Eulerian streaming velocity,

$$V_{Er}(r, \theta) = \langle v_r^{(2)} \rangle = \sum_{l=1}^{\infty} V_{Erl}(r) P_l(\mu), \qquad (47)$$

$$V_{E\theta}(r, \theta) = \langle v_\theta^{(2)} \rangle = \sum_{l=1}^{\infty} V_{E\theta l}(r) P_l^1(\mu), \qquad (48)$$

where

$$V_{Erl}(r) = \Phi_l'(r) - \frac{l(l+1)}{r} \Psi_l(r), \qquad (49)$$

$$V_{E\theta l}(r) = \frac{\Phi_l(r) - \Psi_l(r)}{r} - \Psi_l'(r). \qquad (50)$$

According to Eqs. (B12) and (C18), $\Phi_l'(r)$ and $\Psi_l'(r)$ are calculated by

$$\Phi_l'(r) = -\frac{(l+1)C_{1l}(r)}{r^{l+2}} + l r^{l-1} C_{2l}(r), \qquad (51)$$

$$\Psi_l'(r) = -\frac{(l-1)C_{3l}(r)}{r^l} - \frac{(l+1)C_{4l}(r)}{r^{l+2}}$$
$$+ l r^{l-1} C_{5l}(r) + (l+2) r^{l+1} C_{6l}(r), \qquad (52)$$

where the functions $C_{1l}(r)$–$C_{6l}(r)$ are given by Eqs. (B13), (B14), and (C20)–(C23).

Note that in Eq. (47), we have dropped the term with $l = 0$. This term is a function of r alone and hence it can be represented as the gradient of some function. The curl of the gradient is zero, which means that such a term cannot produce vorticity and hence it does not contribute to acoustic streaming, which is known to be a vortex circulatory flow.
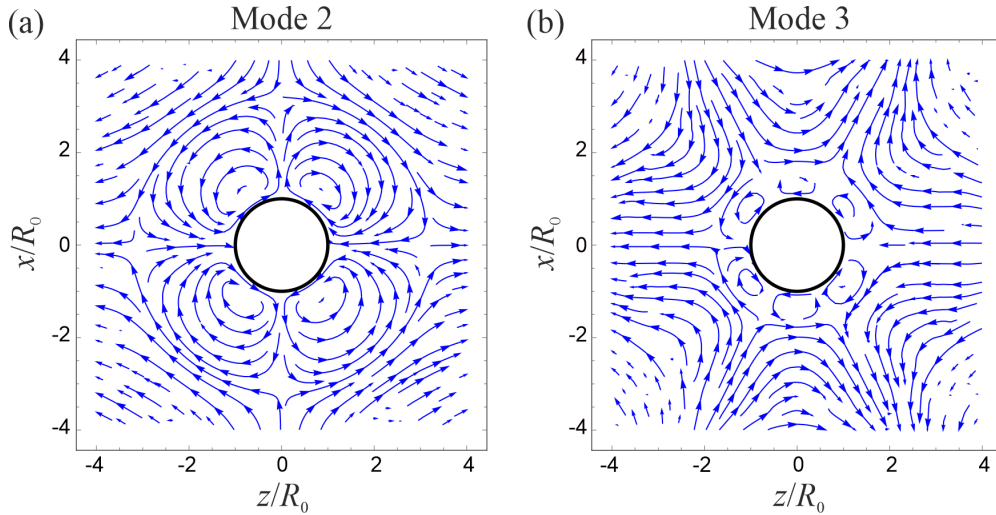
FIG. 6. Streamline patterns at (a) $\eta_p = 0.029$ Pa s, $\lambda_M = 10^{-6}$ s; (b) $\eta_p = 0.009$ Pa s, $\lambda_M = 10^{-5}$ s. The driving is a 100 kHz, 10 kPa plane traveling wave. The particle radius is $R_0 = 50 \ \mu$m.

The components of the Lagrangian streaming velocity, which determine the velocity of fluid particles, are calculated by

$$V_{Lr}(r, \theta) = V_{Er}(r, \theta) + V_{Sr}(r, \theta), \qquad (53)$$

$$V_{L\theta}(r, \theta) = V_{E\theta}(r, \theta) + V_{S\theta}(r, \theta), \qquad (54)$$

where $V_{Sr}(r, \theta)$ and $V_{S\theta}(r, \theta)$ denote the components of the Stokes drift velocity [26], which are calculated in Appendix F and are given by Eqs. (F6) and (F7).

The driving wave generates a stationary flow even if the particle is absent. If it is necessary to eliminate this flow from the Eulerian streaming, $C_{1l}(r)$–$C_{6l}(r)$ should be calculated as said at the end of Appendix E. In order to eliminate a similar part from the Stokes drift velocity, one should follow guidelines given at the end of Appendix F. As a result, we get a part of acoustic streaming that is generated by the particle and absent if the particle is absent. It is just this streaming that is of interest to us in the present study.

III. SIMULATIONS

Figure 2 shows the magnitude of the linear scattering coefficients a_n and b_n, which are given by the equations derived in Appendix A. The coefficients were calculated for a polystyrene particle [27] with the equilibrium radius $R_0 = 50 \ \mu$m, excited by a plane traveling wave with a frequency of 100 kHz and an acoustic pressure amplitude of 10 kPa. Two surrounding fluids were considered: pure water (shown by circles) and a water solution of polyethylene oxide (PEO) [28–32] (shown by triangles). Note that such polymer solutions are also known as polyethylene glycol (PEG).

We use the PEO solution in our simulations because such solutions are widely used in microfluidics [33,34]. Viscometric properties of aqueous solutions of PEO vary in a wide range depending on the concentration of PEO in water and the molecular mass and/or chain length of the used type of PEO [28–32]. In microfluidic applications, these properties are

changed depending on the aim of an application. According to the literature, the relaxation time can be from nanoseconds to milliseconds and more. For example, in experiments of Tian *et al.* [33] on the separation of microparticles, the relaxation time of a PEO solution used was estimated to be 0.078–0.619 ms. The viscosity of concentrated aqueous solutions of PEO (10–50 mass %) with high molecular masses (∼8000) can reach 1 Pa s [30]. However, in most microfluidic applications, such high concentrations and molecular masses, and hence such high viscosities, are not used. The viscosity is usually varied from several mPa s to several tens mPa s. These data have determined the choice of the parameters in our simulations.

The calculations were carried out at the following material parameters: $\rho_s = 1050$ kg/m^3, $E = 0.32 \times 10^{10}$ Pa, $\nu = 0.35$, $\rho_0 = 1000$ kg/m^3, $c = 1500$ m/s, $\eta_f = 0.001$ Pa s, $\zeta_f = 0$, $\eta_p = 0.009$ Pa s (the total shear viscosity is 0.01 Pa s), $\lambda_M = 10^{-6}$ s, and $\zeta_p = 0$ (we set this parameter equal to zero because currently there is no information in the literature about its value).

As follows from Fig. 2, the addition of PEO in water does not practically change the values of a_n, whereas the values of b_n become considerably smaller. It is also seen that for both pure water and the PEO solution, the coefficients rapidly decrease with increasing n. In particular, $a_4/a_3 \sim 10^{-5}$ and $b_4/b_3 \sim 10^{-3}$. This result is a consequence of the general physical law that the intensity of scattering decreases with increasing the order of scattering. Note also that in microfluidic applications, we deal with solid particles whose size is small compared to the acoustic wavelength, which means the absence of resonance effects. This fact suggests that the infinite sums, which appear in the solutions for the acoustic streaming, can be truncated at, for example, $n = 3$ without a noticeable loss of accuracy. This approximation is used in further simulations. The images of different vibration modes can be found in Refs. [35–38].

Results presented in this section illustrate the acoustic streaming produced by the particle, which is defined as the total streaming minus the streaming produced by the driving
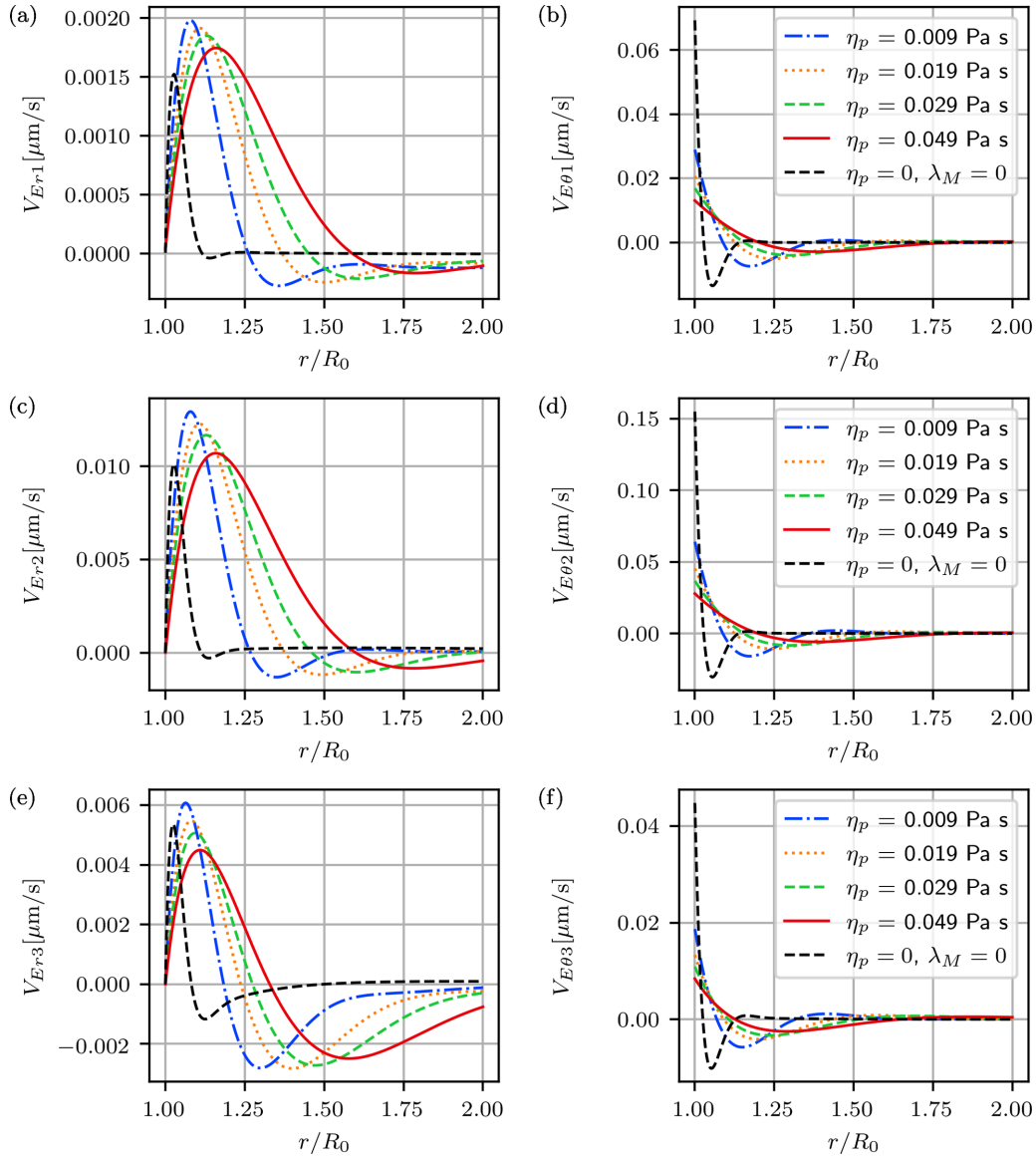
FIG. 7. The r dependence of the components of the Eulerian streaming velocity at different values of η_p for modes with $n = 1,\ 2,\ 3$. The driving is a 100 kHz, 10 kPa plane standing wave. The particle is located halfway between the velocity node and the velocity antinode. The other parameters are as in the traveling wave.

wave in the absence of the particle; see the last paragraph of Sec. II D.

Equations (47) and (48) show that the acoustic streaming is the sum of modes with different angular dependence. In what follows, we consider the first three modes since they are dominant.

Figure 3 demonstrates streamlines of the Lagrangian streaming produced by the particle in a plane traveling wave. The simulations were made for the PEO solution with the parameters indicated above.

Figures 4 and 5 illustrate the behavior of the components of the Eulerian streaming velocity at different values of η_p and λ_M, the other parameters being the same as in Fig. 3. For comparison, results at $\lambda_M = \eta_p = 0$, which correspond to the solvent Newtonian fluid (water), are also presented. As one can see, with increasing η_p, the magnitude of the velocity peak decreases, the peak is shifted to larger r, and its width

becomes broader. In other words, one can say that the spatial domain occupied by the streaming expands. The result that the streaming velocity magnitude decreases with increasing polymer viscosity may look strange, since one expects that increasing viscosity should result in a larger momentum transferred to the fluid. Note, however, that, as pointed out by Lighthill [7], the presence of viscosity in a fluid does lead to velocity gradients that drive streaming. However, at the same time, the viscosity adds resistance to the streaming motion of the fluid. Therefore, a higher viscosity does not always mean faster streaming.

The effect of increasing λ_M, Fig. 5, which corresponds to increasing elasticity, is less unambiguous. When λ_M is changed from 10^{-9} to 10^{-5} s, the magnitude of the velocity peak increases, the peak is shifted to smaller r, and its width becomes narrower. For greater λ_M, the curves for the PEO solution approach those for pure water, which is
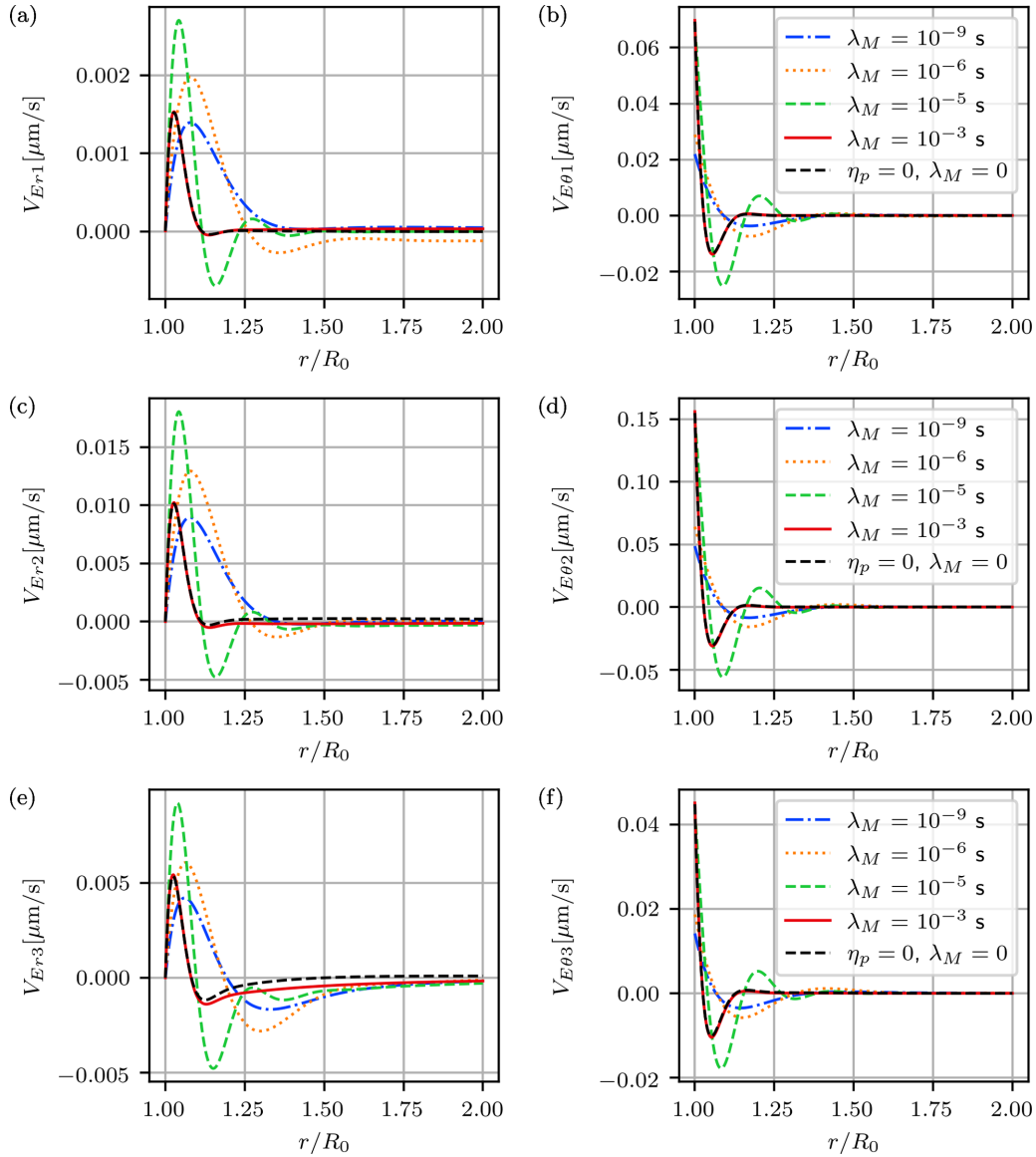
FIG. 8. The r dependence of the components of the Eulerian streaming velocity at different values of λ_M for modes with $n = 1,\ 2,\ 3$. The driving is a 100 kHz, 10 kPa plane standing wave. The particle is located halfway between the velocity node and the velocity antinode. The other parameters are as in the traveling wave.

expectable in view of Eq. (20). Note that the intensity of the acoustic streaming decreases rapidly with the distance from the particle. Therefore, it makes sense to consider the streaming only in the close proximity of the particle. As follows from our figures, a distance of one particle radius is quite adequate.

The variation of η_p and λ_M can change the pattern of streamlines. Figure 6 provides examples. Figure 6(a) shows that increasing η_p results in the development of strong near-surface vortices in mode 2; cf. Fig. 3(b). Figure 6(b) reveals that increasing λ_M induces near-surface vortices in mode 3; cf. Fig. 3(c).

Figures 7 and 8 illustrate the behavior of the components of the Eulerian streaming velocity produced by the particle in a plane standing wave. The particle is assumed to be located halfway between the velocity node and the velocity antinode, $d = c/(8f)$. The other parameters are as in the traveling wave

considered above. As for the plane traveling wave, the magnitude of the velocity peak decreases while the width of the peak increases with increasing η_p, which means that the streaming begins to occupy a greater spatial domain. The reaction of the streaming velocity to changing λ_M is also similar to that in the traveling wave. Streamline patterns of the Lagrangian streaming produced by the particle in the standing wave appear as those in the traveling wave; see Fig. 3.

Figure 9 illustrates the behavior of the first-order scattered wave and acoustic streaming at different values of $\lambda_M f$. This product characterizes the ratio of the relaxation time of the polymer solution to the period of the driving wave acoustic field. The driving field is a 100 kHz, 10 kPa plane standing wave. The particle is located halfway between the velocity node and the velocity antinode. The particle radius is $R_0 = 50\ \mu$m and its material parameters are as above. In order to extend the viscous boundary layer, we set $\eta_p = 1$ Pa s. Three
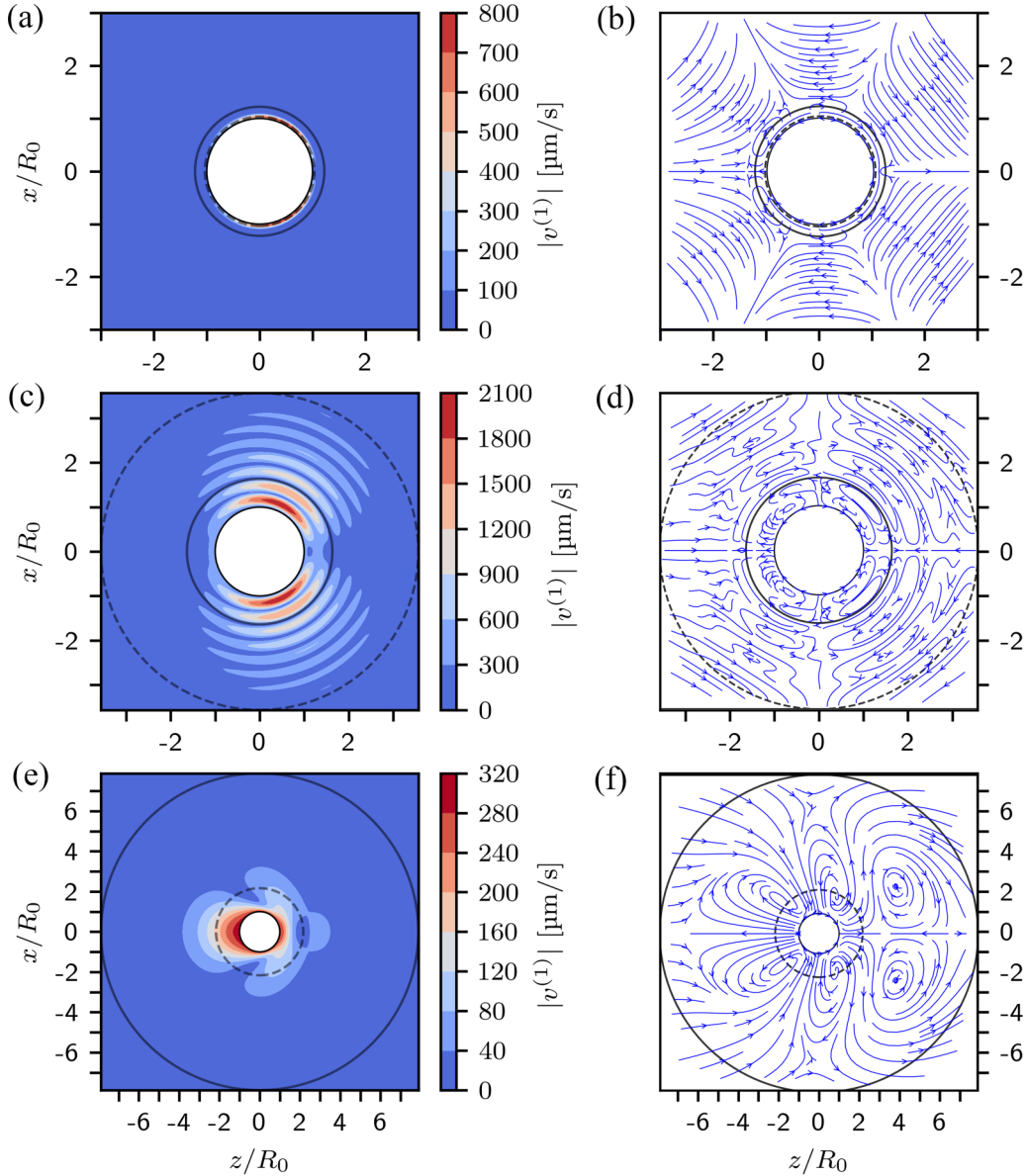
FIG. 9. The first-order scattered wave (left column) and acoustic streaming (right column) at different values of $\lambda_M f$: (a,b) $\lambda_M f = 10^4$; (c,d) $\lambda_M f = 10$; (e,f) $\lambda_M f = 0.01$. The driving is a 100 kHz, 10 kPa plane standing wave. The particle is located halfway between the velocity node and the velocity antinode. The particle radius is $R_0 = 50\ \mu$m, $\eta_p = 1$ Pa s, and the other parameters are as above. The boundary layer thickness is shown by a dashed line and the viscous wavelength is shown by a solid line.

values of the relaxation time are used: $\lambda_M = 10^{-1}$, 10^{-4}, and 10^{-7} s. The boundary layer thickness is shown by a dashed line, while the viscous wavelength is shown by a solid line. Note that the streamline patterns in Fig. 9 show the total acoustic streaming, i.e., the sum of the streaming modes.

For $\lambda_M f = 10^4$, Figs. 9(a) and 9(b), the complex viscosity is approximately equal to the small solvent viscosity $\eta_c \approx \eta_f = 0.001$ Pa s. The viscous boundary layer thickness δ is thus small and the near-surface streaming vortices are confined to a narrow area at the particle surface. In the opposite case, $\lambda_M f = 0.01$, shown in Figs. 9(e) and 9(f), when stresses in the fluid relax fast as compared to the period of the driving wave, $\eta_c \approx \eta_f + \eta_p$. Due to the larger total viscosity, the boundary layer and the streaming vortices spread over a wider

region. Finally, for $\lambda_M f = 10$, Figs. 9(c) and 9(d), the fluid elasticity plays an important role. As opposed for the mostly viscous behavior in the two preceding cases, the boundary layer becomes much larger than the viscous wavelength and viscous waves become visible in the fluid as they are damped out much more slowly, Fig. 9(c). Also, multiple streaming vortices rotating in opposite directions are observed in close proximity of the particle, Fig. 9(d).

IV. CONCLUSIONS

In the present paper, an analytical theory has been developed to model acoustic streaming that is induced by an axisymmetric acoustic wave field around an isotropic solid

particle suspended in a compressible viscoelastic fluid. The particle was assumed to undergo pulsation, translation, and shape deformations of all orders. The fluid motion was described by the compressible Oldroyd-B model. No restrictions were imposed on the particle size with respect to the acoustic wavelength and the viscous penetration depth. The obtained analytical solutions were used to carry out numerical simulations for the acoustic streaming produced by the particle in a plane traveling wave and a plane standing wave.

APPENDIX A: CALCULATION OF THE COEFFICIENTS OF THE FIRST-ORDER SOLUTIONS

In order to calculate the coefficients a_n, b_n, $\widehat{a}_n$, and $\widehat{b}_n$, we apply boundary conditions at the surface of the particle, which are given by

$$v_r^{(1)} = \frac{\partial u_r}{\partial t} \quad \text{at } r = R_0, \tag{A1}$$

$$v_\theta^{(1)} = \frac{\partial u_\theta}{\partial t} \quad \text{at } r = R_0, \tag{A2}$$

$$s_f^{(1)} = s_s \quad \text{at } r = R_0, \tag{A3}$$

$$\tau_f^{(1)} = \tau_s \quad \text{at } r = R_0, \tag{A4}$$

where R_0 is the equilibrium radius of the particle; u_r, u_θ, $v_r^{(1)}$, and $v_\theta^{(1)}$ are given by Eqs. (14), (15), (33), and (34); s_s and τ_s are the normal and tangential stresses in the solid; and $s_f^{(1)}$

and $\tau_f^{(1)}$ are the first-order normal and tangential stresses in the fluid.

The normal stress in the solid is calculated by [14]

$$s_s = \frac{E\nu}{(1 - 2\nu)(1 + \nu)}\nabla \cdot \boldsymbol{u} + \frac{E}{1 + \nu}\frac{\partial u_r}{\partial r}. \tag{A5}$$

On substitution of Eqs. (8), (9), (11), and (14) into Eq. (A5), one obtains

$$s_s = \frac{E e^{-i\omega t}}{(1 + \nu)r^2} \sum_{n=0}^{\infty} \left\{ \widehat{a}_n k_1^2 r^2 \left[j_n''(k_1 r) + \frac{\nu j_n(k_1 r)}{2\nu - 1} \right] \right. \\ \left. - n(n + 1)\widehat{b}_n[k_2 r j_n'(k_2 r) - j_n(k_2 r)] \right\} P_n(\mu). \tag{A6}$$

The tangential stress in the solid is calculated by

$$\tau_s = \frac{E}{2(1 + \nu)}\left(\frac{1}{r}\frac{\partial u_r}{\partial \theta} + \frac{\partial u_\theta}{\partial r} - \frac{u_\theta}{r}\right). \tag{A7}$$

Substituting Eqs. (14) and (15) into Eq. (A7) yields

$$\tau_s = \frac{E e^{-i\omega t}}{2(1 + \nu)r^2} \sum_{n=1}^{\infty} \left\{ 2\widehat{a}_n[k_1 r j_n'(k_1 r) - j_n(k_1 r)] \right. \\ \left. + \widehat{b}_n\left[(2 - n^2 - n)j_n(k_2 r) - k_2^2 r^2 j_n''(k_2 r)\right]\right\} P_n^1(\mu). \tag{A8}$$

From Eqs. (6) and (18), one obtains that the first-order stress in the fluid is defined by

$$\boldsymbol{\sigma}^{(1)} = -p^{(1)}\boldsymbol{I} + \eta_c\left[\nabla \boldsymbol{v}^{(1)} + (\nabla \boldsymbol{v}^{(1)})^T - \tfrac{2}{3}(\nabla \cdot \boldsymbol{v}^{(1)})\boldsymbol{I}\right] + \zeta_c(\nabla \cdot \boldsymbol{v}^{(1)})\boldsymbol{I}, \tag{A9}$$

whence it follows that the first-order normal stress is calculated by

$$s_f^{(1)} = -p^{(1)} + 2\eta_c\frac{\partial v_r^{(1)}}{\partial r} + \left(\zeta_c - \frac{2\eta_c}{3}\right)\nabla \cdot \boldsymbol{v}^{(1)}, \tag{A10}$$

where, according to Eqs. (16), (21), and (23),

$$p^{(1)} = \frac{i\rho_0 c^2 k_f^2}{\omega}\big(\varphi_{\text{ac}} + \varphi_{\text{sc}}^{(1)}\big). \tag{A11}$$

Substitution of Eqs. (28), (30), (33), (35), and (A11) into Eq. (A10) yields

$$s_f^{(1)} = \frac{e^{-i\omega t}}{r^2} \sum_{n=0}^{\infty} P_n(\mu)\left\{ A_n k_f^2 r^2 \left[\left(\frac{2\eta_c}{3} - \zeta_c - \frac{i\rho_0 c^2}{\omega}\right)j_n(k_f r) + 2\eta_c j_n''(k_f r)\right] + a_n k_f^2 r^2 \left[\left(\frac{2\eta_c}{3} - \zeta_c - \frac{i\rho_0 c^2}{\omega}\right) \right.\right. \\ \left.\left. \times h_n^{(1)}(k_f r) + 2\eta_c h_n^{(1)\prime\prime}(k_f r)\right] + 2n(n + 1)b_n\eta_c\big[h_n^{(1)}(k_v r) - k_v r h_n^{(1)\prime}(k_v r)\big]\right\}. \tag{A12}$$

From Eq. (A9) it follows that the first-order tangential stress in the fluid is calculated by

$$\tau_f^{(1)} = \eta_c\left(\frac{1}{r}\frac{\partial v_r^{(1)}}{\partial \theta} + \frac{\partial v_\theta^{(1)}}{\partial r} - \frac{v_\theta^{(1)}}{r}\right), \tag{A13}$$

which, on substitution of Eqs. (33)–(36), gives

$$\tau_f^{(1)} = \frac{\eta_c e^{-i\omega t}}{r^2} \sum_{n=1}^{\infty} P_n^1(\mu)\left\{2A_n[k_f r j_n'(k_f r) - j_n(k_f r)] + 2a_n\big[k_f r h_n^{(1)\prime}(k_f r) - h_n^{(1)}(k_f r)\big] \right. \\ \left. + b_n\big[(2 - n^2 - n)h_n^{(1)}(k_v r) - k_v^2 r^2 h_n^{(1)\prime\prime}(k_v r)\big]\right\}. \tag{A14}$$

On substitution of Eqs. (14), (15), (33)–(36), (A6), (A8), (A12), and (A14) into Eqs. (A1)–(A4), one obtains for the coefficients a_0 and $\widehat{a}_0$,

$$a_0 = \frac{A_0}{D_0} \left\{ \frac{E k_f x_1^2 j_1(x_f)}{1+\nu} \left[j_0''(x_1) - \frac{\nu j_0(x_1)}{1-2\nu} \right] + i\omega k_1 x_f^2 j_1(x_1) \left[2\eta_c j_0''(x_f) - \left(\frac{i\rho_0 c^2}{\omega} + \zeta_c - \frac{2\eta_c}{3} \right) j_0(x_f) \right] \right\}, \quad \text{(A15)}$$

$$\widehat{a}_0 = \frac{A_0 k_f x_f^2}{D_0} \left\{ h_1^{(1)}(x_f) \left[\left(\frac{i\rho_0 c^2}{\omega} + \zeta_c - \frac{2\eta_c}{3} \right) j_0(x_f) - 2\eta_c j_0''(x_f) \right] \right.$$
$$\left. + j_1(x_f) \left[2\eta_c h_0^{(1)''}(x_f) - \left(\frac{i\rho_0 c^2}{\omega} + \zeta_c - \frac{2\eta_c}{3} \right) h_0^{(1)}(x_f) \right] \right\}, \quad \text{(A16)}$$

where $x_f = k_f R_0$, $x_1 = k_1 R_0$, and D_0 is given by

$$D_0 = \frac{E k_f x_1^2 h_1^{(1)}(x_f)}{1+\nu} \left[\frac{\nu j_0(x_1)}{1-2\nu} - j_0''(x_1) \right] + i\omega k_1 x_f^2 j_1(x_1) \left[\left(\frac{i\rho_0 c^2}{\omega} + \zeta_c - \frac{2\eta_c}{3} \right) h_0^{(1)}(x_f) - 2\eta_c h_0^{(1)''}(x_f) \right]. \quad \text{(A17)}$$

The coefficients with $n \geqslant 1$ are calculated by

$$a_n = \frac{\text{Det}[M_1]}{\text{Det}[M]}, \quad b_n = \frac{\text{Det}[M_2]}{\text{Det}[M]}, \quad \widehat{a}_n = \frac{\text{Det}[M_3]}{\text{Det}[M]}, \quad \widehat{b}_n = \frac{\text{Det}[M_4]}{\text{Det}[M]}, \quad \text{(A18)}$$

where M is the square matrix with elements given by Eqs. (A19)–(A22), M_m is the matrix M in which the mth column is replaced with the terms given by Eq. (A23), and $\text{Det}[M]$ denotes the determinant of the matrix M.

$$m_{11} = x_f h_n^{(1)'}(x_f), \quad m_{12} = -n(n+1)h_n^{(1)}(x_v), \quad m_{13} = i\omega x_1 j_n'(x_1), \quad m_{14} = -i\omega n(n+1)j_n(x_2), \quad \text{(A19)}$$

$$m_{21} = h_n^{(1)}(x_f), \quad m_{22} = -h_n^{(1)}(x_v) - x_v h_n^{(1)'}(x_v), \quad m_{23} = i\omega j_n(x_1), \quad m_{24} = -i\omega[j_n(x_2) + x_2 j_n'(x_2)], \quad \text{(A20)}$$

$$m_{31} = x_f^2 \left[2\eta_c h_n^{(1)''}(x_f) - \left(\frac{i\rho_0 c^2}{\omega} + \zeta_c - \frac{2\eta_c}{3} \right) h_n^{(1)}(x_f) \right], \quad m_{32} = 2n(n+1)\eta_c \left[h_n^{(1)}(x_v) - x_v h_n^{(1)'}(x_v) \right],$$

$$m_{33} = \frac{E x_1^2}{1+\nu} \left[\frac{\nu j_n(x_1)}{1-2\nu} - j_n''(x_1) \right], \quad m_{34} = \frac{n(n+1)E}{1+\nu} [x_2 j_n'(x_2) - j_n(x_2)], \quad \text{(A21)}$$

$$m_{41} = 2\eta_c \left[x_f h_n^{(1)'}(x_f) - h_n^{(1)}(x_f) \right], \quad m_{42} = \eta_c \left[(2-n^2-n)h_n^{(1)}(x_v) - x_v^2 h_n^{(1)''}(x_v) \right],$$

$$m_{43} = \frac{E}{1+\nu} [j_n(x_1) - x_1 j_n'(x_1)], \quad m_{44} = \frac{E}{2(1+\nu)} \left[x_2^2 j_n''(x_2) - (2-n^2-n)j_n(x_2) \right], \quad \text{(A22)}$$

$$n_1 = -A_n x_f j_n'(x_f), \quad n_2 = -A_n j_n(x_f), \quad n_3 = A_n x_f^2 \left[\left(\frac{i\rho_0 c^2}{\omega} + \zeta_c - \frac{2\eta_c}{3} \right) j_n(x_f) - 2\eta_c j_n''(x_f) \right],$$

$$n_4 = 2A_n \eta_c [j_n(x_f) - x_f j_n'(x_f)]. \quad \text{(A23)}$$

Here, $x_v = k_v R_0$ and $x_2 = k_2 R_0$.

APPENDIX B: CALCULATION OF Φ

Φ obeys Eq. (43), which can be written as

$$\nabla^2 \Phi = \frac{1}{2\omega} \text{Re} \boldsymbol{\nabla} \cdot \left(i k_f^{2*} \varphi^{(1)*} \boldsymbol{v}^{(1)} \right) = \frac{1}{2\omega} \text{Re} \left\{ i k_f^{2*} \left[\frac{1}{r^2} \frac{\partial}{\partial r} \left(r^2 \varphi^{(1)*} v_r^{(1)} \right) + \frac{1}{r\sin\theta} \frac{\partial}{\partial \theta} \left(\varphi^{(1)*} v_\theta^{(1)} \sin\theta \right) \right] \right\}, \quad \text{(B1)}$$

where "Re" means "the real part of" and the asterisk denotes the complex conjugate.

From Eqs. (28) and (30), it follows that $\varphi^{(1)} = \varphi_{\text{ac}} + \varphi_{\text{sc}}^{(1)}$ is given by

$$\varphi^{(1)} = e^{-i\omega t} \sum_{n=0}^{\infty} \varphi_n(r) P_n(\mu), \quad \text{(B2)}$$

where

$$\varphi_n(r) = A_n j_n(k_f r) + a_n h_n^{(1)}(k_f r). \quad \text{(B3)}$$

Substitution of Eqs. (33), (34), and (B2) into Eq. (B1) yields

$$\nabla^2 \Phi = \frac{1}{2\omega} \text{Re} \left\{ \sum_{n,m=0}^{\infty} [F_{nm}(r) - m(m+1)G_{nm}(r)]P_n(\mu)P_m(\mu) + \sum_{n,m=1}^{\infty} \frac{m(m+1)}{2m+1} G_{nm}(r) \right.$$
$$\left. \times \sum_{k=1}^{[(n+1)/2]} (2n-4k+3)[P_{m-1}(\mu)P_{n-2k+1}(\mu) - P_{m+1}(\mu)P_{n-2k+1}(\mu)] \right\}, \tag{B4}$$

where $[\cdots]$ in the upper bound of the sum means the integer part of an expression inside the brackets and

$$F_{nm}(r) = \frac{ik_f^{2*}}{r} [2\varphi_n^*(r)V_{rm}(r) + r\varphi_n^{*\prime}(r)V_{rm}(r) + r\varphi_n^*(r)V_{rm}'(r)], \tag{B5}$$

$$G_{nm}(r) = \frac{ik_f^{2*}}{r} \varphi_n^*(r)V_{\theta m}(r). \tag{B6}$$

In order to obtain the present form of Eq. (B4), Eqs. (G1)–(G6) have been used to transform expressions with Legendre polynomials.

The right-hand side of Eq. (B4) can be expanded as follows:

$$\nabla^2 \Phi = \sum_{l=0}^{\infty} \alpha_l(r)P_l(\mu), \tag{B7}$$

where the expansion coefficients $\alpha_l(r)$ are calculated by

$$\alpha_l(r) = \frac{2l+1}{2} \int_{-1}^{1} f(r,\mu)P_l(\mu)d\mu, \tag{B8}$$

with $f(r,\mu)$ denoting the function on the right-hand side of Eq. (B4). The calculation of $\alpha_l(r)$ yields

$$\alpha_l(r) = \frac{2l+1}{2\omega} \text{Re} \left\{ \sum_{n=0}^{\infty} \sum_{m=|l-n|}^{l+n} \frac{(C_{l0n0}^{m0})^2}{2m+1} [F_{nm}(r) - m(m+1)G_{nm}(r)] + \sum_{n=1}^{\infty} \sum_{m=1}^{[(n+1)/2]} \sum_{k=|l-(n-2m+1)|}^{l+n-2m+1} \frac{(2n-4m+3)(C_{l0(n-2m+1)0}^{k0})^2}{2k+1} \right.$$
$$\left. \times \left[\frac{(k+1)(k+2)}{2k+3} G_{n(k+1)}(r) - \frac{k(k-1)}{2k-1} G_{n(k-1)}(r) \right] \right\}, \tag{B9}$$

where $C_{l_1m_1l_2m_2}^{LM}$ are the Clebsch-Gordan coefficients [39,40]. To obtain Eq. (B9), we have used Eqs. (G17)–(G19), and the properties of the Clebsch-Gordan coefficients [40], which state that $C_{l_1m_1l_2m_2}^{LM}$ is nonzero only if the following conditions are met: $m_1 + m_2 = M, l_1 + l_2 - L \geqslant 0, l_1 - l_2 + L \geqslant 0, -l_1 + l_2 + L \geqslant 0$.

Equation (B7) suggests that Φ should be sought as

$$\Phi = \sum_{l=0}^{\infty} \Phi_l(r)P_l(\mu). \tag{B10}$$

Substitution of Eq. (B10) into Eq. (B7) yields

$$\frac{d^2\Phi_l}{dr^2} + \frac{2}{r}\frac{d\Phi_l}{dr} - \frac{l(l+1)}{r^2}\Phi_l = \alpha_l(r). \tag{B11}$$

Equation (B11) is solved by the method of variation of constants [41], which gives

$$\Phi_l(r) = \frac{C_{1l}(r)}{r^{l+1}} + C_{2l}(r)r^l. \tag{B12}$$

According to the above method, $C_{1l}(r)$ and $C_{2l}(r)$ are calculated by

$$C_{1l}(r) = C_{1l0} - \frac{1}{2l+1} \int_{R_0}^{r} s^{l+2}\alpha_l(s)ds, \tag{B13}$$

$$C_{2l}(r) = C_{2l0} + \frac{1}{2l+1} \int_{R_0}^{r} s^{1-l}\alpha_l(s)ds, \tag{B14}$$

where C_{1l0} and C_{2l0} are constants, which are calculated in Appendix E.

APPENDIX C: CALCULATION OF Ψ

Ψ obeys Eq. (44). Let us transform the right-hand side of this equation.

We begin with the expression $\langle \boldsymbol{v}^{(1)} \boldsymbol{\nabla} \cdot \boldsymbol{v}^{(1)} + \boldsymbol{v}^{(1)} \cdot \boldsymbol{\nabla} \boldsymbol{v}^{(1)} \rangle$. The radial and tangential components of this expression are given by

$$\langle \boldsymbol{v}^{(1)} \boldsymbol{\nabla} \cdot \boldsymbol{v}^{(1)} + \boldsymbol{v}^{(1)} \cdot \boldsymbol{\nabla} \boldsymbol{v}^{(1)} \rangle_r = \frac{1}{2} \mathrm{Re} \left\{ v_r^{(1)} \frac{\partial v_r^{(1)*}}{\partial r} + \frac{v_\theta^{(1)}}{r} \frac{\partial v_r^{(1)*}}{\partial \theta} - \frac{v_\theta^{(1)} v_\theta^{(1)*}}{r} - v_r^{(1)} k_f^{2*} \varphi^{(1)*} \right\}, \tag{C1}$$

$$\langle \boldsymbol{v}^{(1)} \boldsymbol{\nabla} \cdot \boldsymbol{v}^{(1)} + \boldsymbol{v}^{(1)} \cdot \boldsymbol{\nabla} \boldsymbol{v}^{(1)} \rangle_\theta = \frac{1}{2} \mathrm{Re} \left\{ v_r^{(1)} \frac{\partial v_\theta^{(1)*}}{\partial r} + \frac{v_\theta^{(1)}}{r} \frac{\partial v_\theta^{(1)*}}{\partial \theta} + \frac{v_\theta^{(1)} v_r^{(1)*}}{r} - v_\theta^{(1)} k_f^{2*} \varphi^{(1)*} \right\}. \tag{C2}$$

Substituting Eqs. (33), (34), and (B2) into Eq. (C1) and using Eq. (G8), one obtains

$$\langle \boldsymbol{v}^{(1)} \boldsymbol{\nabla} \cdot \boldsymbol{v}^{(1)} + \boldsymbol{v}^{(1)} \cdot \boldsymbol{\nabla} \boldsymbol{v}^{(1)} \rangle_r = \frac{1}{2} \mathrm{Re} \left\{ \sum_{n,m=0}^{\infty} V_{rn}(r) \left[V_{rm}'^*(r) - k_f^{2*} \varphi_m^*(r) \right] P_n(\mu) P_m(\mu) + \sum_{n,m=1}^{\infty} \frac{m(m+1)}{2m+1} \frac{V_{\theta n}(r) [V_{rm}^*(r) - V_{\theta m}^*(r)]}{r} \right.$$
$$\left. \times \sum_{k=1}^{[(n+1)2]} (2n - 4k + 3) [P_{m-1}(\mu) P_{n-2k+1}(\mu) - P_{m+1}(\mu) P_{n-2k+1}(\mu)] \right\}, \tag{C3}$$

where $[\cdots]$ in the upper bound of the sum means the integer part of an expression inside the brackets.

The right-hand side of Eq. (C3) can be expanded as follows:

$$\langle \boldsymbol{v}^{(1)} \boldsymbol{\nabla} \cdot \boldsymbol{v}^{(1)} + \boldsymbol{v}^{(1)} \cdot \boldsymbol{\nabla} \boldsymbol{v}^{(1)} \rangle_r = \sum_{l=0}^{\infty} \beta_l(r) P_l(\mu), \tag{C4}$$

where, as in Eq. (B8), we use Eqs. (G17)–(G19) in order to calculate the expansion coefficients $\beta_l(r)$,

$$\beta_l(r) = \frac{2l+1}{2} \mathrm{Re} \left(\sum_{n=0}^{\infty} \sum_{m=|l-n|}^{l+n} \frac{\left(C_{l0n0}^{m0}\right)^2}{2m+1} V_{rn}(r) \left[V_{rm}'^*(r) - k_f^{2*} \varphi_m^*(r) \right] \right.$$
$$+ \sum_{n=1}^{\infty} \frac{V_{\theta n}(r)}{r} \sum_{m=1}^{[(n+1)/2]} \sum_{k=|l-(n-2m+1)|}^{l+n-2m+1} \frac{(2n-4m+3)\left(C_{l0(n-2m+1)0}^{k0}\right)^2}{2k+1}$$
$$\left. \times \left\{ \frac{(k+1)(k+2)}{2k+3} [V_{r(k+1)}^*(r) - V_{\theta(k+1)}^*(r)] - \frac{k(k-1)}{2k-1} [V_{r(k-1)}^*(r) - V_{\theta(k-1)}^*(r)] \right\} \right). \tag{C5}$$

Substituting Eqs. (33), (34), and (B2) into Eq. (C2) and using Eq. (G9), one obtains

$$\langle \boldsymbol{v}^{(1)} \boldsymbol{\nabla} \cdot \boldsymbol{v}^{(1)} + \boldsymbol{v}^{(1)} \cdot \boldsymbol{\nabla} \boldsymbol{v}^{(1)} \rangle_\theta = \frac{1}{2} \mathrm{Re} \left(\sum_{\substack{n=0 \\ m=1}}^{\infty} \left\{ V_{rn}(r) V_{\theta m}'^*(r) + \frac{V_{\theta m}(r)[V_{rn}^*(r) - n^2 V_{\theta n}^*(r)]}{r} - k_f^{2*} V_{\theta m}(r) \varphi_n^*(r) \right\} P_n(\mu) P_m^1(\mu) \right.$$
$$\left. + \sum_{\substack{n=2 \\ m=1}}^{\infty} \sum_{k=1}^{[n/2]} (2n - 4k + 1) \frac{V_{\theta n}^*(r) V_{\theta m}(r)}{r} P_{n-2k}(\mu) P_m^1(\mu) \right). \tag{C6}$$

The right-hand side of Eq. (C6) can be expanded as follows:

$$\langle \boldsymbol{v}^{(1)} \boldsymbol{\nabla} \cdot \boldsymbol{v}^{(1)} + \boldsymbol{v}^{(1)} \cdot \boldsymbol{\nabla} \boldsymbol{v}^{(1)} \rangle_\theta = \sum_{l=1}^{\infty} \gamma_l(r) P_l^1(\mu), \tag{C7}$$

where the expansion coefficients $\gamma_l(r)$ are calculated by

$$\gamma_l = \frac{2l+1}{2l(l+1)} \int_{-1}^{1} f(r,\mu) P_l^1(\mu) d\mu, \tag{C8}$$

with $f(r, \mu)$ denoting the function on the right-hand side of Eq. (C6). With the help of Eqs. (G22) and (G23), the calculation of $\gamma_l(r)$ yields

$$
\gamma_l(r) = \frac{2l+1}{2\sqrt{l(l+1)}} \mathrm{Re} \left(\sum_{n=0}^{\infty} \sum_{\substack{m=|n-l| \\ m\geqslant 1}}^{n+l} \frac{\sqrt{m(m+1)} C_{n0l0}^{m0} C_{n0l1}^{m1}}{2m+1} \left\{ V_{rn}(r) V_{\theta m}^{\prime *}(r) + V_{\theta m}(r) \left[\frac{V_{rn}^{*}(r) - n^2 V_{\theta n}^{*}(r)}{r} - k_f^{2*} \varphi_n^{*}(r) \right] \right\} \right.
$$

$$
\left. + \sum_{n=2}^{\infty} \frac{V_{\theta n}^{*}(r)}{r} \sum_{m=1}^{[n/2]} \sum_{\substack{k=|n-2m-l| \\ k\geqslant 1}}^{n-2m+l} \frac{(2n-4m+1)\sqrt{k(k+1)} C_{(n-2m)0l0}^{k0} C_{(n-2m)0l1}^{k1}}{2k+1} V_{\theta k}(r) \right). \tag{C9}
$$

Thus, according to Eqs. (C4) and (C7),

$$
\langle \boldsymbol{v}^{(1)} \boldsymbol{\nabla} \cdot \boldsymbol{v}^{(1)} + \boldsymbol{v}^{(1)} \cdot \boldsymbol{\nabla} \boldsymbol{v}^{(1)} \rangle = \boldsymbol{e}_r \sum_{l=0}^{\infty} \beta_l(r) P_l(\mu) + \boldsymbol{e}_{\theta} \sum_{l=1}^{\infty} \gamma_l(r) P_l^1(\mu). \tag{C10}
$$

From Eq. (C10), one obtains

$$
\boldsymbol{\nabla} \times \langle \boldsymbol{v}^{(1)} \boldsymbol{\nabla} \cdot \boldsymbol{v}^{(1)} + \boldsymbol{v}^{(1)} \cdot \boldsymbol{\nabla} \boldsymbol{v}^{(1)} \rangle = \frac{\boldsymbol{e}_{\varepsilon}}{r} \sum_{l=1}^{\infty} [\gamma_l(r) + r\gamma_l'(r) - \beta_l(r)] P_l^1(\mu). \tag{C11}
$$

Let now us consider the term $\langle \boldsymbol{\nabla} \cdot \mathbf{T} \rangle$ of Eq. (44). Since the calculation of $\langle \boldsymbol{\nabla} \cdot \mathbf{T} \rangle$ is very cumbersome, it is carried out in Appendix D. The final result is

$$
\langle \boldsymbol{\nabla} \cdot \mathbf{T} \rangle = \boldsymbol{e}_r \sum_{l=0}^{\infty} D_l^{(r)}(r) P_l(\mu) + \boldsymbol{e}_{\theta} \sum_{l=1}^{\infty} D_l^{(\theta)}(r) P_l^1(\mu), \tag{C12}
$$

where $D_l^{(r)}(r)$ and $D_l^{(\theta)}(r)$ are defined by Eqs. (D42) and (D47).

From Eq. (C12), one obtains

$$
\boldsymbol{\nabla} \times \langle \boldsymbol{\nabla} \cdot \mathbf{T} \rangle = \frac{\boldsymbol{e}_{\varepsilon}}{r} \sum_{l=1}^{\infty} \left[D_l^{(\theta)}(r) + r D_l^{(\theta)\prime}(r) - D_l^{(r)}(r) \right] P_l^1(\mu). \tag{C13}
$$

Substitution of Eqs. (C11) and (C13) into Eq. (44) yields

$$
\nabla^4 \boldsymbol{\Psi} = -\frac{\boldsymbol{e}_{\varepsilon}}{(\eta_f + \eta_p) r} \sum_{l=1}^{\infty} \left\{ \rho_0 [\gamma_l(r) + r\gamma_l'(r) - \beta_l(r)] + \lambda_M \left[D_l^{(\theta)}(r) + r D_l^{(\theta)\prime}(r) - D_l^{(r)}(r) \right] \right\} P_l^1(\mu). \tag{C14}
$$

A solution to Eq. (C14) is sought as

$$
\boldsymbol{\Psi} = \boldsymbol{e}_{\varepsilon} \sum_{l=1}^{\infty} \Psi_l(r) P_l^1(\mu). \tag{C15}
$$

Substituting Eq. (C15) into Eq. (C14) gives the following equation for $\Psi_l(r)$:

$$
\Psi_l^{IV} + \frac{4}{r} \Psi_l''' - \frac{2l(l+1)}{r^2} \Psi_l'' + \frac{l(l+1)(l^2+l-2)}{r^4} \Psi_l = E_l(r), \tag{C16}
$$

where

$$
E_l(r) = -\frac{1}{(\eta_f + \eta_p) r} \left\{ \rho_0 [\gamma_l(r) + r\gamma_l'(r) - \beta_l(r)] + \lambda_M \left[D_l^{(\theta)}(r) + r D_l^{(\theta)\prime}(r) - D_l^{(r)}(r) \right] \right\}. \tag{C17}
$$

Equation (C16) is solved by the method of variation of constants [32]. As a result, one obtains

$$
\Psi_l(r) = \frac{C_{3l}(r)}{r^{l-1}} + \frac{C_{4l}(r)}{r^{l+1}} + r^l C_{5l}(r) + r^{l+2} C_{6l}(r), \tag{C18}
$$

where the functions $C_{3l}(r)$–$C_{6l}(r)$ obey the following set of equations:

$$
r^{-(l-1)} C_{3l}' + r^{-(l+1)} C_{4l}' + r^l C_{5l}' + r^{l+2} C_{6l}' = 0,
$$

$$
(l-1) r^{-l} C_{3l}' + (l+1) r^{-(l+2)} C_{4l}' - l r^{l-1} C_{5l}' - (l+2) r^{l+1} C_{6l}' = 0,
$$

$$
l(l-1) r^{-(l+1)} C_{3l}' + (l+1)(l+2) r^{-(l+3)} C_{4l}' + l(l-1) r^{l-2} C_{5l}' + (l+1)(l+2) r^l C_{6l}' = 0,
$$

$$
l(l^2-1) r^{-(l+2)} C_{3l}' + (l+1)(l+2)(l+3) r^{-(l+4)} C_{4l}' - l(l-1)(l-2) r^{l-3} C_{5l}' - l(l+1)(l+2) r^{l-1} C_{6l}' = -E_l(r). \tag{C19}
$$

It follows from system (C19) that

$$C_{3l}(r) = C_{3l0} + \frac{1}{2(2l-1)(2l+1)} \int_{R_0}^{r} s^{l+2} E_l(s) ds, \tag{C20}$$

$$C_{4l}(r) = C_{4l0} - \frac{1}{2(2l+1)(2l+3)} \int_{R_0}^{r} s^{l+4} E_l(s) ds, \tag{C21}$$

$$C_{5l}(r) = C_{5l0} - \frac{1}{2(2l-1)(2l+1)} \int_{R_0}^{r} s^{3-l} E_l(s) ds, \tag{C22}$$

$$C_{6l}(r) = C_{6l0} + \frac{1}{2(2l+1)(2l+3)} \int_{R_0}^{r} s^{1-l} E_l(s) ds, \tag{C23}$$

where C_{3l0}–C_{6l0} are constants, which are calculated in Appendix E.

APPENDIX D: CALCULATION OF $\langle \nabla \cdot \mathbf{T} \rangle$

The tensor $\mathbf{T}$, which is defined by Eq. (39), can be represented as

$$\mathrm{T}_{ik} = v_j^{(1)} \nabla_j \tau_{ik}^{(1)} - 2\tau_{ij}^{(1)} v_{jk}^{(1)}, \tag{D1}$$

where, according to Eq. (40), the tensor $\tau_{ik}^{(1)}$ is given by

$$\tau_{ik}^{(1)} = \frac{2\eta_p}{1 - i\omega\lambda_M} v_{ik}^{(1)} + \frac{\zeta_p - 2\eta_p/3}{1 - i\omega\lambda_M} (\nabla \cdot \mathbf{v}^{(1)}) \delta_{ik}, \tag{D2}$$

$v_{ik}^{(1)}$ is the rate-of-strain tensor [14], δ_{ik} is the Kronecker delta, and summation over repeated indices is implied.

In the case of axial symmetry, the nonzero components of $v_{ik}^{(1)}$ in spherical coordinates are given by [14]

$$v_{rr}^{(1)} = \frac{\partial v_r^{(1)}}{\partial r}, \quad v_{\theta\theta}^{(1)} = \frac{1}{r}\left(v_r^{(1)} + \frac{\partial v_\theta^{(1)}}{\partial \theta}\right), \quad v_{\varepsilon\varepsilon}^{(1)} = \frac{v_r^{(1)} + v_\theta^{(1)} \cot\theta}{r}, \quad v_{r\theta}^{(1)} = \frac{1}{2}\left(\frac{1}{r}\frac{\partial v_r^{(1)}}{\partial \theta} + \frac{\partial v_\theta^{(1)}}{\partial r} - \frac{v_\theta^{(1)}}{r}\right), \tag{D3}$$

whence it follows that the nonzero components of $\tau_{ik}^{(1)}$ are given by

$$\tau_{rr}^{(1)} = \frac{2\eta_p}{1 - i\omega\lambda_M} \frac{\partial v_r^{(1)}}{\partial r} + \frac{\zeta_p - 2\eta_p/3}{1 - i\omega\lambda_M} (\nabla \cdot \mathbf{v}^{(1)}), \tag{D4}$$

$$\tau_{\theta\theta}^{(1)} = \frac{2\eta_p}{1 - i\omega\lambda_M} \left(\frac{v_r^{(1)}}{r} + \frac{1}{r}\frac{\partial v_\theta^{(1)}}{\partial \theta}\right) + \frac{\zeta_p - 2\eta_p/3}{1 - i\omega\lambda_M} (\nabla \cdot \mathbf{v}^{(1)}), \tag{D5}$$

$$\tau_{\varepsilon\varepsilon}^{(1)} = \frac{2\eta_p}{1 - i\omega\lambda_M} \left(\frac{v_r^{(1)}}{r} + \frac{v_\theta^{(1)} \cot\theta}{r}\right) + \frac{\zeta_p - 2\eta_p/3}{1 - i\omega\lambda_M} (\nabla \cdot \mathbf{v}^{(1)}), \tag{D6}$$

$$\tau_{r\theta}^{(1)} = \frac{\eta_p}{1 - i\omega\lambda_M} \left(\frac{1}{r}\frac{\partial v_r^{(1)}}{\partial \theta} + \frac{\partial v_\theta^{(1)}}{\partial r} - \frac{v_\theta^{(1)}}{r}\right). \tag{D7}$$

As a first step, we calculate the tensor $\langle \mathrm{T}_{ik} \rangle$, which is defined by

$$\langle \mathrm{T}_{ik} \rangle = \tfrac{1}{2} \mathrm{Re}\left\{v_j^{(1)*} \nabla_j \tau_{ik}^{(1)} - 2\tau_{ij}^{(1)} v_{jk}^{(1)*}\right\}. \tag{D8}$$

Let us begin with the calculation of the term $\tau_{ij}^{(1)} v_{jk}^{(1)*}$. Substitution of $v_{jk}^{(1)*}$ in Eq. (D2) yields

$$\tau_{ij}^{(1)} v_{jk}^{(1)*} = \frac{2\eta_p}{1 - i\omega\lambda_M} v_{ij}^{(1)} v_{jk}^{(1)*} + \frac{\zeta_p - 2\eta_p/3}{1 - i\omega\lambda_M} (\nabla \cdot \mathbf{v}^{(1)}) v_{ik}^{(1)*}. \tag{D9}$$

Substituting Eqs. (D3)–(D7) into Eq. (D9), one obtains that the nonzero components of $\tau_{ij}^{(1)} v_{jk}^{(1)*}$ in spherical coordinates are given by

$$\left[\tau_{ij}^{(1)} v_{jk}^{(1)*}\right]_{rr} = \frac{2\eta_p}{1 - i\omega\lambda_M} \left[\left|\frac{\partial v_r^{(1)}}{\partial r}\right|^2 + \frac{1}{4}\left|\frac{1}{r}\frac{\partial v_r^{(1)}}{\partial \theta} + \frac{\partial v_\theta^{(1)}}{\partial r} - \frac{v_\theta^{(1)}}{r}\right|^2\right] + \frac{\zeta_p - 2\eta_p/3}{1 - i\omega\lambda_M} (\nabla \cdot \mathbf{v}^{(1)}) \frac{\partial v_r^{(1)*}}{\partial r}, \tag{D10}$$

$$\left[\tau_{ij}^{(1)} v_{jk}^{(1)*}\right]_{\theta\theta} = \frac{2\eta_p}{1 - i\omega\lambda_M} \left[\left|\frac{v_r^{(1)}}{r} + \frac{1}{r}\frac{\partial v_\theta^{(1)}}{\partial \theta}\right|^2 + \frac{1}{4}\left|\frac{1}{r}\frac{\partial v_r^{(1)}}{\partial \theta} + \frac{\partial v_\theta^{(1)}}{\partial r} - \frac{v_\theta^{(1)}}{r}\right|^2\right] + \frac{\zeta_p - 2\eta_p/3}{1 - i\omega\lambda_M} (\nabla \cdot \mathbf{v}^{(1)}) \left(\frac{v_r^{(1)*}}{r} + \frac{1}{r}\frac{\partial v_\theta^{(1)*}}{\partial \theta}\right), \tag{D11}$$

$$\left[\tau_{ij}^{(1)}v_{jk}^{(1)*}\right]_{\varepsilon\varepsilon} = \frac{2\eta_p}{1-i\omega\lambda_M}\left|\frac{v_r^{(1)}}{r} + \frac{v_\theta^{(1)}\cot\theta}{r}\right|^2 + \frac{\zeta_p - 2\eta_p/3}{1-i\omega\lambda_M}(\boldsymbol{\nabla}\cdot\boldsymbol{v}^{(1)})\left(\frac{v_r^{(1)*}}{r} + \frac{v_\theta^{(1)*}\cot\theta}{r}\right), \tag{D12}$$

$$\left[\tau_{ij}^{(1)}v_{jk}^{(1)*}\right]_{r\theta} = \frac{\eta_p}{1-i\omega\lambda_M}\left[\frac{\partial v_r^{(1)}}{\partial r}\left(\frac{1}{r}\frac{\partial v_r^{(1)*}}{\partial\theta} + \frac{\partial v_\theta^{(1)*}}{\partial r} - \frac{v_\theta^{(1)*}}{r}\right) + \left(\frac{1}{r}\frac{\partial v_r^{(1)}}{\partial\theta} + \frac{\partial v_\theta^{(1)}}{\partial r} - \frac{v_\theta^{(1)}}{r}\right)\left(\frac{v_r^{(1)*}}{r} + \frac{1}{r}\frac{\partial v_\theta^{(1)*}}{\partial\theta}\right)\right]$$
$$+ \frac{\zeta_p - 2\eta_p/3}{2(1-i\omega\lambda_M)}(\boldsymbol{\nabla}\cdot\boldsymbol{v}^{(1)})\left(\frac{1}{r}\frac{\partial v_r^{(1)*}}{\partial\theta} + \frac{\partial v_\theta^{(1)*}}{\partial r} - \frac{v_\theta^{(1)*}}{r}\right). \tag{D13}$$

We proceed to the calculation of the term $v_j^{(1)*}\nabla_j\tau_{ik}^{(1)}$,

$$v_j^{(1)*}\nabla_j\tau_{ik}^{(1)} = \frac{2\eta_p}{1-i\omega\lambda_M}v_j^{(1)*}\nabla_j v_{ik}^{(1)} + \frac{\zeta_p - 2\eta_p/3}{1-i\omega\lambda_M}\delta_{ik}(\boldsymbol{v}^{(1)*}\cdot\boldsymbol{\nabla})(\boldsymbol{\nabla}\cdot\boldsymbol{v}^{(1)}). \tag{D14}$$

To calculate Eq. (D14), we use tensor analysis in orthogonal curvilinear coordinates; see, for example, Ref. [42]. According to the above branch of science, $\nabla_j v_{ik}^{(1)}$ is calculated by

$$\nabla_j v_{ik}^{(1)} = \frac{\partial v_{ik}^{(1)}}{\partial x^j} - v_{lk}^{(1)}\Gamma_{ij}^l - v_{il}^{(1)}\Gamma_{kj}^l. \tag{D15}$$

where x^j denotes the contravariant coordinates of the position vector $\boldsymbol{r}$ and Γ_{ij}^l stands for the Christoffel symbols.

In the case of spherical coordinates and axial symmetry, Eq. (D15) has the following nonzero components:

$$\left[\nabla_1 v_{11}^{(1)}\right]_{rrr} = \frac{\partial v_{rr}^{(1)}}{\partial r}, \quad \left[\nabla_1 v_{22}^{(1)}\right]_{r\theta\theta} = \frac{\partial v_{\theta\theta}^{(1)}}{\partial r}, \quad \left[\nabla_1 v_{33}^{(1)}\right]_{r\varepsilon\varepsilon} = \frac{\partial v_{\varepsilon\varepsilon}^{(1)}}{\partial r}, \quad \left[\nabla_1 v_{12}^{(1)}\right]_{rr\theta} = \frac{\partial v_{r\theta}^{(1)}}{\partial r}, \tag{D16}$$

$$\left[\nabla_2 v_{11}^{(1)}\right]_{\theta rr} = \frac{1}{r}\frac{\partial v_{rr}^{(1)}}{\partial\theta} - \frac{2v_{r\theta}^{(1)}}{r}, \quad \left[\nabla_2 v_{22}^{(1)}\right]_{\theta\theta\theta} = \frac{1}{r}\frac{\partial v_{\theta\theta}^{(1)}}{\partial\theta} + \frac{2v_{r\theta}^{(1)}}{r}, \tag{D17}$$

$$\left[\nabla_2 v_{33}^{(1)}\right]_{\theta\varepsilon\varepsilon} = \frac{1}{r}\frac{\partial v_{\varepsilon\varepsilon}^{(1)}}{\partial\theta}, \quad \left[\nabla_2 v_{12}^{(1)}\right]_{\theta r\theta} = \frac{1}{r}\frac{\partial v_{r\theta}^{(1)}}{\partial\theta} + \frac{v_{rr}^{(1)} - v_{\theta\theta}^{(1)}}{r}. \tag{D18}$$

It follows from Eqs. (D16)–(D18) that the tensor $v_j^{(1)*}\nabla_j v_{ik}^{(1)}$ has the following components:

$$\left[v_j^{(1)*}\nabla_j v_{ik}^{(1)}\right]_{rr} = v_r^{(1)*}\frac{\partial^2 v_r^{(1)}}{\partial r^2} + \frac{v_\theta^{(1)*}}{r}\left(\frac{\partial^2 v_r^{(1)}}{\partial r\partial\theta} - \frac{1}{r}\frac{\partial v_r^{(1)}}{\partial\theta} - \frac{\partial v_\theta^{(1)}}{\partial r} + \frac{v_\theta^{(1)}}{r}\right), \tag{D19}$$

$$\left[v_j^{(1)*}\nabla_j v_{ik}^{(1)}\right]_{\theta\theta} = \frac{v_r^{(1)*}}{r}\left(\frac{\partial^2 v_\theta^{(1)}}{\partial r\partial\theta} + \frac{\partial v_r^{(1)}}{\partial r} - \frac{1}{r}\frac{\partial v_\theta^{(1)}}{\partial\theta} - \frac{v_r^{(1)}}{r}\right) + \frac{v_\theta^{(1)*}}{r}\left(\frac{1}{r}\frac{\partial^2 v_\theta^{(1)}}{\partial\theta^2} + \frac{2}{r}\frac{\partial v_r^{(1)}}{\partial\theta} + \frac{\partial v_\theta^{(1)}}{\partial r} - \frac{v_\theta^{(1)}}{r}\right), \tag{D20}$$

$$\left[v_j^{(1)*}\nabla_j v_{ik}^{(1)}\right]_{\varepsilon\varepsilon} = \frac{v_r^{(1)*}}{r}\left(\frac{\partial v_r^{(1)}}{\partial r} + \cot\theta\frac{\partial v_\theta^{(1)}}{\partial r} - \frac{v_r^{(1)} + v_\theta^{(1)}\cot\theta}{r}\right) + \frac{v_\theta^{(1)*}}{r^2}\left(\frac{\partial v_r^{(1)}}{\partial\theta} + \cot\theta\frac{\partial v_\theta^{(1)}}{\partial\theta} - \frac{v_\theta^{(1)}}{\sin^2\theta}\right), \tag{D21}$$

$$\left[v_j^{(1)*}\nabla_j v_{ik}^{(1)}\right]_{r\theta} = \frac{v_r^{(1)*}}{2}\left(\frac{1}{r}\frac{\partial^2 v_r^{(1)}}{\partial r\partial\theta} + \frac{\partial^2 v_\theta^{(1)}}{\partial r^2} - \frac{1}{r^2}\frac{\partial v_r^{(1)}}{\partial\theta} - \frac{1}{r}\frac{\partial v_\theta^{(1)}}{\partial r} + \frac{v_\theta^{(1)}}{r^2}\right)$$
$$+ \frac{v_\theta^{(1)*}}{2r}\left(\frac{1}{r}\frac{\partial^2 v_r^{(1)}}{\partial\theta^2} + \frac{\partial^2 v_\theta^{(1)}}{\partial r\partial\theta} + 2\frac{\partial v_r^{(1)}}{\partial r} - \frac{3}{r}\frac{\partial v_\theta^{(1)}}{\partial\theta} - \frac{2v_r^{(1)}}{r}\right). \tag{D22}$$

Substitution of Eqs. (D10)–(D13) and (D19)–(D22) into Eq. (D8) gives nonzero components of the tensor $\langle T_{ik}\rangle$,

$$\langle T_{rr}\rangle = \frac{1}{2}\mathrm{Re}\left\{\frac{2\eta_p}{1-i\omega\lambda_M}\left[v_r^{(1)*}\frac{\partial^2 v_r^{(1)}}{\partial r^2} + \frac{v_\theta^{(1)*}}{r}\left(\frac{\partial^2 v_r^{(1)}}{\partial r\partial\theta} - \frac{1}{r}\frac{\partial v_r^{(1)}}{\partial\theta} - \frac{\partial v_\theta^{(1)}}{\partial r} + \frac{v_\theta^{(1)}}{r}\right)\right.\right.$$
$$\left.\left. - 2\left|\frac{\partial v_r^{(1)}}{\partial r}\right|^2 - \frac{1}{2}\left|\frac{1}{r}\frac{\partial v_r^{(1)}}{\partial\theta} + \frac{\partial v_\theta^{(1)}}{\partial r} - \frac{v_\theta^{(1)}}{r}\right|^2\right] + \frac{\zeta_p - 2\eta_p/3}{1-i\omega\lambda_M}\left[(\boldsymbol{v}^{(1)*}\cdot\boldsymbol{\nabla})(\boldsymbol{\nabla}\cdot\boldsymbol{v}^{(1)}) - 2(\boldsymbol{\nabla}\cdot\boldsymbol{v}^{(1)})\frac{\partial v_r^{(1)*}}{\partial r}\right]\right\}, \tag{D23}$$

$$\langle T_{\theta\theta}\rangle = \frac{1}{2}\mathrm{Re}\left\{\frac{2\eta_p}{1-i\omega\lambda_M}\left[\frac{v_r^{(1)*}}{r}\left(\frac{\partial^2 v_\theta^{(1)}}{\partial r\partial\theta} + \frac{\partial v_r^{(1)}}{\partial r} - \frac{1}{r}\frac{\partial v_\theta^{(1)}}{\partial\theta} - \frac{v_r^{(1)}}{r}\right)\right.\right.$$
$$\left. + \frac{v_\theta^{(1)*}}{r}\left(\frac{1}{r}\frac{\partial^2 v_\theta^{(1)}}{\partial\theta^2} + \frac{2}{r}\frac{\partial v_r^{(1)}}{\partial\theta} + \frac{\partial v_\theta^{(1)}}{\partial r} - \frac{v_\theta^{(1)}}{r}\right) - 2\left|\frac{v_r^{(1)}}{r} + \frac{1}{r}\frac{\partial v_\theta^{(1)}}{\partial\theta}\right|^2 - \frac{1}{2}\left|\frac{1}{r}\frac{\partial v_r^{(1)}}{\partial\theta} + \frac{\partial v_\theta^{(1)}}{\partial r} - \frac{v_\theta^{(1)}}{r}\right|^2\right]$$
$$\left. + \frac{\zeta_p - 2\eta_p/3}{1-i\omega\lambda_M}\left[(\boldsymbol{v}^{(1)*}\cdot\boldsymbol{\nabla})(\boldsymbol{\nabla}\cdot\boldsymbol{v}^{(1)}) - 2(\boldsymbol{\nabla}\cdot\boldsymbol{v}^{(1)})\left(\frac{v_r^{(1)*}}{r} + \frac{1}{r}\frac{\partial v_\theta^{(1)*}}{\partial\theta}\right)\right]\right\}, \tag{D24}$$

$$\langle T_{\varepsilon\varepsilon}\rangle = \frac{1}{2}\mathrm{Re}\Bigg\{\frac{2\eta_p}{1-i\omega\lambda_M}\Bigg[\frac{v_r^{(1)*}}{r}\Big(\frac{\partial v_r^{(1)}}{\partial r}+\cot\theta\,\frac{\partial v_\theta^{(1)}}{\partial r}-\frac{v_r^{(1)}+v_\theta^{(1)}\cot\theta}{r}\Big)$$

$$+\frac{v_\theta^{(1)*}}{r^2}\Big(\frac{\partial v_r^{(1)}}{\partial\theta}+\cot\theta\,\frac{\partial v_\theta^{(1)}}{\partial\theta}-\frac{v_\theta^{(1)}}{\sin^2\theta}\Big)-2\Big|\frac{v_r^{(1)}}{r}+\frac{v_\theta^{(1)}\cot\theta}{r}\Big|^2\Bigg]$$

$$+\frac{\zeta_p-2\eta_p/3}{1-i\omega\lambda_M}\Big[(\boldsymbol{v}^{(1)*}\cdot\boldsymbol{\nabla})(\boldsymbol{\nabla}\cdot\boldsymbol{v}^{(1)})-2(\boldsymbol{\nabla}\cdot\boldsymbol{v}^{(1)})\Big(\frac{v_r^{(1)*}}{r}+\frac{v_\theta^{(1)*}\cot\theta}{r}\Big)\Big]\Bigg]\Bigg\},\tag{D25}$$

$$\langle T_{r\theta}\rangle = \frac{1}{2}\mathrm{Re}\Bigg\{\frac{2\eta_p}{1-i\omega\lambda_M}\Bigg[\frac{v_r^{(1)*}}{2}\Big(\frac{1}{r}\frac{\partial^2 v_r^{(1)}}{\partial r\partial\theta}+\frac{\partial^2 v_\theta^{(1)}}{\partial r^2}-\frac{1}{r^2}\frac{\partial v_r^{(1)}}{\partial\theta}-\frac{1}{r}\frac{\partial v_\theta^{(1)}}{\partial r}+\frac{v_\theta^{(1)}}{r^2}\Big)$$

$$+\frac{v_\theta^{(1)*}}{2r}\Big(\frac{1}{r}\frac{\partial^2 v_r^{(1)}}{\partial\theta^2}+\frac{\partial^2 v_\theta^{(1)}}{\partial r\partial\theta}+2\frac{\partial v_r^{(1)}}{\partial r}-\frac{3}{r}\frac{\partial v_\theta^{(1)}}{\partial\theta}-\frac{2v_r^{(1)}}{r}\Big)-\frac{\partial v_r^{(1)}}{\partial r}\Big(\frac{1}{r}\frac{\partial v_r^{(1)*}}{\partial\theta}+\frac{\partial v_\theta^{(1)*}}{\partial r}-\frac{v_\theta^{(1)*}}{r}\Big)$$

$$-\Big(\frac{1}{r}\frac{\partial v_r^{(1)}}{\partial\theta}+\frac{\partial v_\theta^{(1)}}{\partial r}-\frac{v_\theta^{(1)}}{r}\Big)\Big(\frac{v_r^{(1)*}}{r}+\frac{1}{r}\frac{\partial v_\theta^{(1)*}}{\partial\theta}\Big)\Bigg]-\frac{\zeta_P-2\eta_p/3}{1-i\omega\lambda_M}(\boldsymbol{\nabla}\cdot\boldsymbol{v}^{(1)})\Big(\frac{1}{r}\frac{\partial v_r^{(1)*}}{\partial\theta}+\frac{\partial v_\theta^{(1)*}}{\partial r}-\frac{v_\theta^{(1)*}}{r}\Big)\Bigg\}.\tag{D26}$$

Substitution of Eqs. (33), (34), and (B2) into Eqs. (D23)–(D26) results in

$$\langle T_{rr}\rangle = \mathrm{Re}\Bigg[\sum_{n,m=0}^{\infty}P_n(\mu)P_m(\mu)\Bigg\{\frac{\eta_p}{1-i\omega\lambda_M}[V_{rn}^*(r)V''_{rm}(r)-2V_{rn}'^*(r)V'_{rm}(r)]+\frac{k_f^2(\zeta_p-2\eta_p/3)}{2(1-i\omega\lambda_M)}[2\varphi_n(r)V_{rm}'^*(r)-\varphi'_n(r)V_{rm}^*(r)]\Bigg\}$$

$$+\sum_{n,m=1}^{\infty}P_n^1(\mu)P_m^1(\mu)\Bigg(\frac{\eta_p}{1-i\omega\lambda_M}\Bigg\{\frac{V_{\theta n}^*(r)}{r}\Big[V'_{rm}(r)-V'_{\theta m}(r)+\frac{V_{\theta m}(r)-V_{rm}(r)}{r}\Big]$$

$$-\frac{1}{2}\Big[V'_{\theta n}(r)+\frac{V_{rn}(r)-V_{\theta n}(r)}{r}\Big]\Big[V_{\theta m}'^*(r)+\frac{V_{rm}^*(r)-V_{\theta m}^*(r)}{r}\Big]\Bigg\}-\frac{k_f^2(\zeta_p-2\eta_p/3)}{2(1-i\omega\lambda_M)}\frac{\varphi_n(r)V_{\theta m}^*(r)}{r}\Bigg)\Bigg],\tag{D27}$$

$$\langle T_{\theta\theta}\rangle = \mathrm{Re}\Bigg[\sum_{n,m=0}^{\infty}P_n(\mu)P_m(\mu)\Bigg(\frac{\eta_p}{1-i\omega\lambda_M}\Bigg\{\frac{V_{rn}^*(r)V'_{rm}(r)}{r}-\frac{3V_{rn}^*(r)V_{rm}(r)}{r^2}$$

$$+m^2\Big[\frac{3V_{rn}^*(r)V_{\theta m}(r)+2V_{rn}(r)V_{\theta m}^*(r)}{r^2}-\frac{V_{rn}^*(r)V'_{\theta m}(r)}{r}\Big]+nm(1-m-2nm)\frac{V_{\theta n}^*(r)V_{\theta m}(r)}{r^2}\Bigg\}$$

$$+\frac{k_f^2(\zeta_p-2\eta_p/3)}{2(1-i\omega\lambda_M)}\Bigg\{\frac{2\varphi_n(r)}{r}\Big[V_{rm}^*(r)-m^2V_{\theta m}^*(r)\Big]-\varphi'_n(r)V_{rm}^*(r)\Bigg\}\Bigg)$$

$$+\sum_{n,m=1}^{\infty}P_n^1(\mu)P_m^1(\mu)\Bigg(\frac{\eta_p}{1-i\omega\lambda_M}\Bigg\{\frac{V_{\theta n}^*(r)V'_{\theta m}(r)}{r}+\frac{2V_{\theta n}^*(r)V_{rm}(r)-(m^2+m+1)V_{\theta n}^*(r)V_{\theta m}(r)}{r^2}$$

$$-\frac{1}{2}\Big[V'_{\theta n}(r)+\frac{V_{rn}(r)-V_{\theta n}(r)}{r}\Big]\Big[V_{\theta m}'^*(r)+\frac{V_{rm}^*(r)-V_{\theta m}^*(r)}{r}\Big]\Bigg\}-\frac{k_f^2(\zeta_p-2\eta_p/3)}{2(1-i\omega\lambda_M)}\frac{\varphi_n(r)V_{\theta m}^*(r)}{r}\Bigg)$$

$$+\sum_{\substack{n=2\\m=0}}^{\infty}\sum_{k=1}^{[n/2]}P_m(\mu)P_{n-2k}(\mu)(2n-4k+1)\Bigg(\frac{\eta_p}{1-i\omega\lambda_M}\Bigg\{\frac{V_{rm}^*(r)V'_{\theta n}(r)}{r}-\frac{3V_{rm}^*(r)V_{\theta n}(r)+2V_{rm}(r)V_{\theta n}^*(r)}{r^2}$$

$$+\frac{m(m+1)[2V_{\theta n}(r)V_{\theta m}^*(r)+V_{\theta n}^*(r)V_{\theta m}(r)]}{r^2}\Bigg\}+\frac{k_f^2(\zeta_p-2\eta_p/3)}{1-i\omega\lambda_M}\frac{\varphi_m(r)V_{\theta n}^*(r)}{r}\Bigg)$$

$$+\frac{\eta_p}{1-i\omega\lambda_M}\sum_{\substack{n=2\\m=1}}^{\infty}\sum_{k=1}^{[n/2]}[P_{m-1}(\mu)P_{n-2k}(\mu)-P_{m+1}(\mu)P_{n-2k}(\mu)](2n-4k+1)\frac{m(m+1)}{2m+1}\frac{V_{\theta m}^*(r)V_{\theta(n-1)}(r)}{r^2}\Bigg],\tag{D28}$$

$$\langle T_{\varepsilon\varepsilon}\rangle = \mathrm{Re}\Bigg[\sum_{n,m=0}^{\infty}P_n(\mu)P_m(\mu)\Bigg(\frac{\eta_p}{1-i\omega\lambda_M}\Bigg\{\frac{V_{rn}^*(r)[V'_{rm}(r)-mV'_{\theta m}(r)]}{r}$$

$$+\frac{2V_{rn}(r)[mV_{\theta m}^*(r)-V_{rm}^*(r)]+V_{rn}^*(r)[3mV_{\theta m}(r)-V_{rm}(r)]+nm(m-2)V_{\theta n}^*(r)V_{\theta m}(r)}{r^2}\Bigg\}$$

$$
+ \frac{k_f^2(\zeta_p - 2\eta_p/3)}{2(1 - i\omega\lambda_M)} \left\{ \frac{2\varphi_n(r)[V_{rm}^*(r) - m V_{\theta m}^*(r)]}{r} - \varphi_n'(r)V_{rm}^*(r) \right\} \Bigg)
$$

$$
+ \sum_{n,m=1}^{\infty} P_n^1(\mu)P_m^1(\mu)\left[\frac{\eta_p}{1 - i\omega\lambda_M} \frac{V_{\theta n}^*(r)V_{rm}(r)}{r^2} - \frac{k_f^2(\zeta_p - 2\eta_p/3)}{2(1 - i\omega\lambda_M)} \frac{\varphi_n(r)V_{\theta m}^*(r)}{r} \right]
$$

$$
+ \sum_{\substack{n=2 \\ m=0}}^{\infty} \sum_{k=1}^{[n/2]} P_{n-2k}(\mu)P_m(\mu)(2n - 4k + 1)\Bigg(\frac{\eta_p}{1 - i\omega\lambda_M} \left\{ \frac{V_{\theta n}^*(r)[2V_{rm}(r) + m(m - 2)V_{\theta m}(r)]}{r^2} \right.
$$

$$
+ \frac{3V_{\theta n}(r)[V_{rm}^*(r) - m V_{\theta m}^*(r)]}{r^2} - \frac{V_{rm}^*(r)V_{\theta n}'(r)}{r} \Bigg\} - \frac{k_f^2(\zeta_p - 2\eta_p/3)}{2(1 - i\omega\lambda_M)} \frac{2\varphi_m(r)V_{\theta n}^*(r)}{r} \Bigg)
$$

$$
- \frac{\eta_p}{1 - i\omega\lambda_M} \sum_{n,m=2}^{\infty} \sum_{k=1}^{[n/2]} \sum_{s=1}^{[m/2]} P_{n-2k}(\mu)P_{m-2s}(\mu)(2n - 4k + 1)(2m - 4s + 1)\frac{3V_{\theta n}^*(r)V_{\theta m}(r) + V_{\theta(n-1)}^*(r)V_{\theta(m-1)}(r)}{r^2} \Bigg],
$$

(D29)

$$
\langle \mathrm{T}_{r\theta} \rangle = \mathrm{Re}\Bigg[\sum_{\substack{n=0 \\ m=1}}^{\infty} P_n(\mu)P_m^1(\mu)\Bigg(\frac{\eta_p}{1 - i\omega\lambda_M} \left\{ \frac{V_{rn}^*(r)V_{\theta m}''(r)}{2} - V_{rn}'(r)V_{\theta m}^{*\prime}(r) \right.
$$

$$
+ \frac{V_{rn}^*(r)[V_{rm}'(r) - 3V_{\theta m}'(r)] + 2V_{rn}'(r)[2V_{\theta m}^*(r) - V_{rm}^*(r)] + n^2[2V_{\theta n}^*(r)V_{\theta m}'(r) - V_{\theta m}^*(r)V_{\theta n}'(r)]}{2r}
$$

$$
+ \frac{[V_{rm}(r) - V_{\theta m}(r)][2n^2 V_{\theta n}^*(r) - 3V_{rn}^*(r)] + V_{\theta m}^*(r)[3n^2 V_{\theta n}(r) - (n^2 + 2)V_{rn}(r)]}{2r^2} \Bigg\}
$$

$$
+ \frac{k_f^2(\zeta_p - 2\eta_p/3)}{2(1 - i\omega\lambda_M)} \varphi_n(r)\left[V_{\theta m}^{*\prime}(r) + \frac{V_{rm}^*(r) - V_{\theta m}^*(r)}{r} \right] \Bigg) - \sum_{\substack{n=2 \\ m=1}}^{\infty} \sum_{k=1}^{[n/2]} P_{n-2k}(\mu)P_m^1(\mu)(2n - 4k + 1)\frac{\eta_p}{1 - i\omega\lambda_M}
$$

$$
\times \left[\frac{2V_{\theta n}^*(r)[V_{rm}(r) - V_{\theta m}(r)] + V_{\theta m}^*(r)[3V_{\theta n}(r) - V_{rn}(r)]}{2r^2} + \frac{2V_{\theta n}^*(r)V_{\theta m}'(r) - V_{\theta m}^*(r)V_{\theta n}'(r)}{2r} \right] \Bigg].
$$

(D30)

In Eqs. (D27)–(D30), the transformation of expressions with Legendre polynomials has been carried out by using Eqs. (G1)–(G14).

The right-hand sides of Eqs. (D27)–(D29) can be expanded in $P_l(\mu)$ and the right-hand side of Eq. (D30) can be expanded in $P_l^1(\mu)$. Doing so with the help of Eqs. (G15)–(G23), one obtains

$$
\langle \mathrm{T}_{rr} \rangle = \sum_{l=0}^{\infty} T_l^{(rr)}(r)P_l(\mu),
$$

(D31)

$$
\langle \mathrm{T}_{\theta\theta} \rangle = \sum_{l=0}^{\infty} T_l^{(\theta\theta)}(r)P_l(\mu),
$$

(D32)

$$
\langle \mathrm{T}_{\varepsilon\varepsilon} \rangle = \sum_{l=0}^{\infty} T_l^{(\varepsilon\varepsilon)}(r)P_l(\mu),
$$

(D33)

$$
\langle \mathrm{T}_{r\theta} \rangle = \sum_{l=1}^{\infty} T_l^{(r\theta)}(r)P_l^1(\mu),
$$

(D34)

where the r-dependent functions are calculated by

$$
T_l^{(rr)}(r) = (2l + 1)\mathrm{Re}\sum_{n=0}^{\infty} \sum_{m=|l-n|}^{l+n} \frac{(C_{l0n0}^{m0})^2}{2m + 1}\left\{ \frac{\eta_p}{1 - i\omega\lambda_M}[V_{rn}^*(r)V_{rm}''(r) - 2V_{rn}^{*\prime}(r)V_{rm}'(r)] \right.
$$

$$
+ \frac{k_f^2(\zeta_p - 2\eta_p/3)}{2(1 - i\omega\lambda_M)}[2\varphi_n(r)V_{rm}^{*\prime}(r) - \varphi_n'(r)V_{rm}^*(r)] \Bigg\}
$$

$$
+ (2l + 1)\mathrm{Re}\sum_{n=1}^{\infty} \sum_{m=1}^{[(n+1)/2]} (2n - 4m + 3)\sum_{k=|l-(n-2m+1)|}^{l+n-2m+1} \frac{(C_{l0(n-2m+1)0}^{k0})^2}{2k + 1}
$$

$$\times \left[\frac{(k+1)(k+2)}{2k+3} \left(\frac{\eta_p}{1-i\omega\lambda_M} \left\{ \frac{V_{\theta n}^*(r)}{r} \left[V_{r(k+1)}'(r) - V_{\theta(k+1)}'(r) + \frac{V_{\theta(k+1)}(r) - V_{r(k+1)}(r)}{r} \right] \right. \right. \right.$$

$$\left. \left. -\frac{1}{2} \left[\frac{V_{rn}(r) - V_{\theta n}(r)}{r} + V_{\theta n}'(r) \right] \left[\frac{V_{r(k+1)}^*(r) - V_{\theta(k+1)}^*(r)}{r} + V_{\theta(k+1)}'^*(r) \right] \right\} - \frac{k_f^2(\zeta_p - 2\eta_p/3)}{2(1-i\omega\lambda_M)} \frac{\varphi_n(r) V_{\theta(k+1)}^*(r)}{r} \right)$$

$$- \frac{k(k-1)}{2k-1} \left(\frac{\eta_p}{1-i\omega\lambda_M} \left\{ \frac{V_{\theta n}^*(r)}{r} \left[V_{r(k-1)}'(r) - V_{\theta(k-1)}'(r) + \frac{V_{\theta(k-1)}(r) - V_{r(k-1)}(r)}{r} \right] \right. \right.$$

$$\left. \left. \left. -\frac{1}{2} \left[V_{\theta n}'(r) + \frac{V_{rn}(r) - V_{\theta n}(r)}{r} \right] \left[V_{\theta(k-1)}'^*(r) + \frac{V_{r(k-1)}^*(r) - V_{\theta(k-1)}^*(r)}{r} \right] \right\} - \frac{k_f^2(\zeta_p - 2\eta_p/3)}{2(1-i\omega\lambda_M)} \frac{\varphi_n(r) V_{\theta(k-1)}^*(r)}{r} \right) \right],$$

$$\text{(D35)}$$

$$T_l^{(\theta\theta)}(r) = (2l+1)\text{Re} \sum_{n=0}^{\infty} \sum_{m=|l-n|}^{l+n} \frac{(C_{l0n0}^{m0})^2}{2m+1} \left(\frac{\eta_p}{1-i\omega\lambda_M} \left\{ \frac{V_{rn}^*(r) V_{rm}'(r)}{r} - \frac{3 V_{rn}^*(r) V_{rm}(r)}{r^2} \right. \right.$$

$$\left. + m^2 \left[\frac{3 V_{rn}^*(r) V_{\theta m}(r) + 2 V_{rn}(r) V_{\theta m}^*(r)}{r^2} - \frac{V_{rn}^*(r) V_{\theta m}'(r)}{r} \right] + nm(1-m-2nm) \frac{V_{\theta n}^*(r) V_{\theta m}(r)}{r^2} \right\}$$

$$\left. + \frac{k_f^2(\zeta_p - 2\eta_p/3)}{2(1-i\omega\lambda_M)} \left\{ \frac{2\varphi_n(r)[V_{rm}^*(r) - m^2 V_{\theta m}^*(r)]}{r} - \varphi_n'(r) V_{rm}^*(r) \right\} \right)$$

$$+ (2l+1)\text{Re} \sum_{n=1}^{\infty} \sum_{m=1}^{[(n+1)/2]} (2n-4m+3) \sum_{k=|l-(n-2m+1)|}^{l+n-2m+1} \frac{(C_{l0(n-2m+1)0}^{k0})^2}{2k+1}$$

$$\times \left[\frac{(k+1)(k+2)}{2k+3} \left(\frac{\eta_p}{1-i\omega\lambda_M} \left\{ \frac{2 V_{\theta n}^*(r) V_{r(k+1)}(r)}{r^2} + \frac{V_{\theta n}^*(r) V_{\theta(k+1)}'(r)}{r} - \frac{[1+(k+1)(k+2)] V_{\theta n}^*(r) V_{\theta(k+1)}(r)}{r^2} \right. \right. \right.$$

$$\left. \left. -\frac{1}{2} \left[V_{\theta n}'(r) + \frac{V_{rn}(r) - V_{\theta n}(r)}{r} \right] \left[V_{\theta(k+1)}'^*(r) + \frac{V_{r(k+1)}^*(r) - V_{\theta(k+1)}^*(r)}{r} \right] \right\} - \frac{k_f^2(\zeta_p - 2\eta_p/3)}{2(1-i\omega\lambda_M)} \frac{\varphi_n(r) V_{\theta(k+1)}^*(r)}{r} \right)$$

$$- \frac{k(k-1)}{2k-1} \left(\frac{\eta_p}{1-i\omega\lambda_M} \left\{ \frac{V_{\theta n}^*(r) V_{\theta(k-1)}'(r)}{r} + \frac{2 V_{\theta n}^*(r) V_{r(k-1)}(r) - (k^2-k+1) V_{\theta n}^*(r) V_{\theta(k-1)}(r)}{r^2} \right. \right.$$

$$\left. \left. \left. -\frac{1}{2} \left[V_{\theta n}'(r) + \frac{V_{rn}(r) - V_{\theta n}(r)}{r} \right] \left[V_{\theta(k-1)}'^*(r) + \frac{V_{r(k-1)}^*(r) - V_{\theta(k-1)}^*(r)}{r} \right] \right\} - \frac{k_f^2(\zeta_p - 2\eta_p/3)}{2(1-i\omega\lambda_M)} \frac{\varphi_n(r) V_{\theta(k-1)}^*(r)}{r} \right) \right]$$

$$+ (2l+1)\text{Re} \sum_{n=2}^{\infty} \sum_{m=1}^{[n/2]} (2n-4m+1) \sum_{k=|l-(n-2m)|}^{l+n-2m} \frac{(C_{l0(n-2m)0}^{k0})^2}{2k+1}$$

$$\times \left(\frac{\eta_p}{1-i\omega\lambda_M} \left\{ \frac{V_{rk}^*(r) V_{\theta n}'(r)}{r} - \frac{3 V_{rk}^*(r) V_{\theta n}(r) + 2 V_{rk}(r) V_{\theta n}^*(r)}{r^2} \right. \right.$$

$$\left. + \frac{k(k+1)[2 V_{\theta n}(r) V_{\theta k}^*(r) + V_{\theta n}^*(r) V_{\theta k}(r)]}{r^2} + \frac{(k+1)(k+2)}{2k+3} \frac{V_{\theta(k+1)}^*(r) V_{\theta(n-1)}(r)}{r^2} \right.$$

$$\left. - \frac{k(k-1)}{2k-1} \frac{V_{\theta(k-1)}^*(r) V_{\theta(n-1)}(r)}{r^2} \right\} + \frac{k_f^2(\zeta_p - 2\eta_p/3)}{1-i\omega\lambda_M} \frac{\varphi_k(r) V_{\theta n}^*(r)}{r} \right),$$

$$\text{(D36)}$$

$$T_l^{(\varepsilon\varepsilon)}(r) = (2l+1)\text{Re} \sum_{n=0}^{\infty} \sum_{m=|l-n|}^{l+n} \frac{(C_{l0n0}^{m0})^2}{2m+1} \left(\frac{\eta_p}{1-i\omega\lambda_M} \left\{ \frac{V_{rn}^*(r)[V_{rm}'(r) - m V_{\theta m}'(r)]}{r} \right. \right.$$

$$\left. + \frac{2 V_{rn}(r)[m V_{\theta m}^*(r) - V_{rm}^*(r)] + V_{rn}^*(r)[3m V_{\theta m}(r) - V_{rm}(r)] + nm(m-2) V_{\theta n}^*(r) V_{\theta m}(r)}{r^2} \right\}$$

$$\left. + \frac{k_f^2(\zeta_p - 2\eta_p/3)}{2(1-i\omega\lambda_M)} \left\{ \frac{2\varphi_n(r)[V_{rm}^*(r) - m V_{\theta m}^*(r)]}{r} - \varphi_n'(r) V_{rm}^*(r) \right\} \right)$$

$$+ (2l+1)\text{Re} \sum_{n=1}^{\infty} \sum_{m=1}^{[(n+1)/2]} (2n-4m+3) \sum_{k=|l-(n-2m+1)|}^{l+n-2m+1} \frac{(C_{l0(n-2m+1)0}^{k0})^2}{2k+1}$$

$$\times \left\{ \frac{(k+1)(k+2)}{2k+3} \left[\frac{\eta_p}{1-i\omega\lambda_M} \frac{V_{\theta n}^*(r)V_{r(k+1)}(r)}{r^2} - \frac{k_f^2(\zeta_p - 2\eta_p/3)}{2(1-i\omega\lambda_M)} \frac{\varphi_n(r)V_{\theta(k+1)}^*(r)}{r} \right] \right.$$

$$\left. - \frac{k(k-1)}{2k-1} \left[\frac{\eta_p}{1-i\omega\lambda_M} \frac{V_{\theta n}^*(r)V_{r(k-1)}(r)}{r^2} - \frac{k_f^2(\zeta_p - 2\eta_p/3)}{2(1-i\omega\lambda_M)} \frac{\varphi_n(r)V_{\theta(k-1)}^*(r)}{r} \right] \right\}$$

$$+ (2l+1)\text{Re} \sum_{n=2}^{\infty} \sum_{m=1}^{[n/2]} (2n-4m+1) \sum_{k=|l-(n-2m)|}^{l+n-2m} \frac{\left(C_{l0(n-2m)0}^{k0}\right)^2}{2k+1}$$

$$\times \left(\frac{\eta_p}{1-i\omega\lambda_M} \left\{ \frac{V_{\theta n}^*(r)[2V_{rk}(r) + k(k-2)V_{\theta k}(r)] + 3V_{\theta n}(r)[V_{rk}^*(r) - kV_{\theta k}^*(r)]}{r^2} - \frac{V_{rk}^*(r)V_{\theta n}'(r)}{r} \right\} \right.$$

$$\left. - \frac{k_f^2(\zeta_p - 2\eta_p/3)}{2(1-i\omega\lambda_M)} \frac{2\varphi_k(r)V_{\theta n}^*(r)}{r} \right) - (2l+1)\text{Re} \left[\frac{\eta_p}{1-i\omega\lambda_M} \sum_{n=2}^{\infty} \sum_{m=1}^{[n/2]} (2n-4m+1) \sum_{k=|l-(n-2m)|}^{l+n-2m} \left(C_{l0(n-2m)0}^{k0}\right)^2 \right.$$

$$\left. \times \sum_{q=2+k}^{\infty} \frac{3V_{\theta n}^*(r)V_{\theta q}(r) + V_{\theta(n-1)}^*(r)V_{\theta(q-1)}(r)}{r^2} \sum_{s=1}^{[q/2]} \delta_{k(q-2s)} \right], \tag{D37}$$

$$T_l^{(r\theta)}(r) = \frac{2l+1}{\sqrt{l(l+1)}} \text{Re} \sum_{n=0}^{\infty} \sum_{\substack{m=|n-l| \\ m \geqslant 1}}^{n+l} \frac{\sqrt{m(m+1)}C_{n0l0}^{m0}C_{n0l1}^{m1}}{2m+1} \left(\frac{\eta_p}{1-i\omega\lambda_M} \left\{ \frac{V_{rn}^*(r)V_{\theta m}''(r)}{2} - V_{rn}'(r)V_{\theta m}^{*'}(r) \right. \right.$$

$$+ \frac{V_{rn}^*(r)[V_{rm}'(r) - 3V_{\theta m}'(r)] + 2V_{rn}'[2V_{\theta m}^*(r) - V_{rm}^*(r)] + n^2[2V_{\theta n}^*(r)V_{\theta m}'(r) - V_{\theta m}^*(r)V_{\theta n}'(r)]}{2r}$$

$$\left. + \frac{[V_{rm}(r) - V_{\theta m}(r)][2n^2V_{\theta n}^*(r) - 3V_{rn}^*(r)] + V_{\theta m}^*(r)[3n^2V_{\theta n}(r) - (n^2+2)V_{rn}(r)]}{2r^2} \right\}$$

$$\left. + \frac{k_f^2(\zeta_p - 2\eta_p/3)}{2(1-i\omega\lambda_M)} \varphi_n(r) \left[V_{\theta m}^{*'}(r) + \frac{V_{rm}^*(r) - V_{\theta m}^*(r)}{r} \right] \right)$$

$$- \frac{2l+1}{\sqrt{l(l+1)}} \text{Re} \left(\frac{\eta_p}{1-i\omega\lambda_M} \sum_{n=2}^{\infty} \sum_{m=1}^{[n/2]} (2n-4m+1) \sum_{\substack{k=|n-2m-l| \\ k \geqslant 1}}^{n-2m+l} \frac{\sqrt{k(k+1)}C_{(n-2m)0l0}^{k0}C_{(n-2m)0l1}^{k1}}{2k+1} \right.$$

$$\left. \left\{ \frac{2V_{\theta n}^*(r)[V_{rk}(r) - V_{\theta k}(r)] + V_{\theta k}^*(r)[3V_{\theta n}(r) - V_{rn}(r)]}{2r^2} + \frac{2V_{\theta n}^*(r)V_{\theta k}'(r) - V_{\theta k}^*(r)V_{\theta n}'(r)}{2r} \right\} \right). \tag{D38}$$

The components of $\langle \nabla \cdot \mathbf{T} \rangle$ are calculated by [43]

$$\langle \nabla \cdot \mathbf{T} \rangle_r = \frac{\partial \langle T_{rr} \rangle}{\partial r} + \frac{1}{r} \frac{\partial \langle T_{r\theta} \rangle}{\partial \theta} + \frac{1}{r} (2\langle T_{rr} \rangle + \langle T_{r\theta} \rangle \cot\theta - \langle T_{\theta\theta} \rangle - \langle T_{\varepsilon\varepsilon} \rangle), \tag{D39}$$

$$\langle \nabla \cdot \mathbf{T} \rangle_\theta = \frac{\partial \langle T_{r\theta} \rangle}{\partial r} + \frac{1}{r} \frac{\partial \langle T_{\theta\theta} \rangle}{\partial \theta} + \frac{1}{r} [3\langle T_{r\theta} \rangle + (\langle T_{\theta\theta} \rangle - \langle T_{\varepsilon\varepsilon} \rangle) \cot\theta]. \tag{D40}$$

Substitution of Eqs. (D31)–(D34) into Eq. (D39) yields

$$\langle \nabla \cdot \mathbf{T} \rangle_r = \sum_{l=0}^{\infty} D_l^{(r)}(r) P_l(\mu), \tag{D41}$$

where

$$D_l^{(r)}(r) = T_l^{(rr)'}(r) + \frac{2T_l^{(rr)}(r) - T_l^{(\theta\theta)}(r) - T_l^{(\varepsilon\varepsilon)}(r) - l(l+1)T_l^{(r\theta)}(r)}{r}. \tag{D42}$$

Substitution of Eqs. (D31)–(D34) into Eq. (D40) yields

$$\langle \nabla \cdot \mathbf{T} \rangle_\theta = \sum_{l=1}^{\infty} \left[T_l^{(r\theta)'}(r) + \frac{3T_l^{(r\theta)}(r) + T_l^{(\theta\theta)}(r)}{r} \right] P_l^1(\mu) + \sum_{l=0}^{\infty} \frac{T_l^{(\theta\theta)}(r) - T_l^{(\varepsilon\varepsilon)}(r)}{r} \frac{\mu P_l(\mu)}{\sqrt{1-\mu^2}}. \tag{D43}$$

We use the following expansion:

$$\frac{\mu P_l(\mu)}{\sqrt{1-\mu^2}} = \sum_{n=1}^{\infty} a_{ln} P_n^1(\mu). \tag{D44}$$

The calculation of the coefficients a_{ln} gives

$$a_{ln} = -\frac{\delta_{nl}}{n+1} - \frac{2n+1}{n(n+1)} \sum_{k=1}^{[n/2]} \delta_{(n-2k)l}. \tag{D45}$$

On substitution of Eqs. (D44) and (D45), Eq. (D43) takes the following form:

$$\langle \boldsymbol{\nabla} \cdot \mathbf{T} \rangle_\theta = \sum_{l=1}^{\infty} D_l^{(\theta)}(r) P_l^1(\mu), \tag{D46}$$

where

$$D_l^{(\theta)}(r) = T_l^{(r\theta)'}(r) + \frac{3(l+1)T_l^{(r\theta)}(r) + lT_l^{(\theta\theta)}(r) + T_l^{(\varepsilon\varepsilon)}(r)}{(l+1)r} - \frac{2l+1}{l(l+1)} \sum_{k=1}^{[l/2]} \frac{T_{l-2k}^{(\theta\theta)}(r) - T_{l-2k}^{(\varepsilon\varepsilon)}(r)}{r}. \tag{D47}$$

APPENDIX E: CALCULATION OF THE CONSTANTS C_{1l0}–C_{6l0}

The term C_{1l0}/r^{l+1} in the equation for Φ_l, Eq. (B12), gives the same contribution to the velocity field as the term C_{4l0}/r^{l+1} in the equation for Ψ_l, Eq. (C18), in view of the identity

$$\boldsymbol{\nabla} \times \left[\boldsymbol{e}_\varepsilon P_l^1(\mu) r^{-(l+1)} \right] = -l\boldsymbol{\nabla}[P_l(\mu) r^{-(l+1)}]. \tag{E1}$$

Therefore, in order to remove this doubling, we set

$$C_{1l0} = 0. \tag{E2}$$

This operation is valid because we do not consider the term with $l=0$, which does not contribute to acoustic streaming.

In order to calculate the constants C_{2l0}, C_{5l0}, and C_{6l0}, we use the behavior of the Eulerian streaming velocity, $\boldsymbol{V}_E$, at $r \to \infty$. A part of $\boldsymbol{V}_E$ that is caused by the presence of the particle, i.e., a part that results from the interaction of the first-order scattered wave with itself and with the driving acoustic wave, must tend to zero for $r \to \infty$. From this condition, substituting Eqs. (51), (52), (B12), and (C18) into Eqs. (49) and (50), one obtains

$$C_{2l}^{(sc)}(r) - (l+1)C_{5l}^{(sc)}(r) - (l+1)r^2 C_{6l}^{(sc)}(r) = 0 \quad \text{for} \quad r \to \infty, \tag{E3}$$

$$C_{2l}^{(sc)}(r) - (l+1)C_{5l}^{(sc)}(r) - (l+3)r^2 C_{6l}^{(sc)}(r) = 0 \quad \text{for} \quad r \to \infty, \tag{E4}$$

where the superscript (sc) denotes that only terms with the scattered wave are kept.

Substituting Eqs. (B14), (C22), and (C23) into Eqs. (E3) and (E4) and keeping only terms with the scattered wave, one obtains

$$C_{2l0} = -\frac{1}{2l+1} \int_{R_0}^{\infty} s^{1-l} \big[\alpha_l(s) - \alpha_l^{(ac)}(s) \big] ds, \tag{E5}$$

$$C_{5l0} = \frac{1}{2(2l-1)(2l+1)} \int_{R_0}^{\infty} s^{3-l} \big[E_l(s) - E_l^{(ac)}(s) \big] ds, \tag{E6}$$

$$C_{6l0} = -\frac{1}{2(2l+1)(2l+3)} \int_{R_0}^{\infty} s^{1-l} \big[E_l(s) - E_l^{(ac)}(s) \big] ds, \tag{E7}$$

where the superscript (ac) denotes that $\alpha_l^{(ac)}(s)$ and $E_l^{(ac)}(s)$ are calculated by Eqs. (B9) and (C17) in which only terms with $A_n A_n^*$ are kept. In other words, when $\alpha_l^{(ac)}(s)$ and $E_l^{(ac)}(s)$ are calculated, we drop terms with a_n and b_n in Eqs. (35), (36), and (B3) and set

$$V_{rn}(r) = A_n k_f j_n'(k_f r), \quad V_{\theta n}(r) = A_n j_n(k_f r)/r, \quad \varphi_n(r) = A_n j_n(k_f r). \tag{E8}$$

In order to calculate the constants C_{3l0} and C_{4l0}, boundary conditions at the particle surface are applied, which are specified by

$$V_{Lr} = V_{L\theta} = 0 \quad \text{at} \quad r = R_0. \tag{E9}$$

Substitution of Eqs. (47), (48), (F6), and (F7) into Eq. (E9) yields

$$lR_0^2 C_{3l0} + lC_{4l0} = \frac{R_0^{l+2}}{l+1} V_{Srl}(R_0) + \frac{lR_0^{2l+1}}{l+1} C_{2l0} - lR_0^{2l+1} C_{5l0} - lR_0^{2l+3} C_{6l0}, \tag{E10}$$

$$(l-2)R_0^2 C_{3l0} + l C_{4l0} = (l+1)R_0^{2l+1}C_{5l0} + (l+3)R_0^{2l+3}C_{6l0} - R_0^{2l+1}C_{2l0} - R_0^{l+2}V_{S\theta l}(R_0), \tag{E11}$$

whence it follows that

$$C_{3l0} = \frac{1}{2}\left\{ R_0^l \left[\frac{V_{Srl}(R_0)}{l+1} + V_{S\theta l}(R_0) \right] + (2l+1)R_0^{2l-1}\left(\frac{C_{2l0}}{l+1} - C_{5l0} \right) - (2l+3)R_0^{2l+1}C_{6l0} \right\}, \tag{E12}$$

$$C_{4l0} = \frac{1}{2}\left\{ R_0^{l+2} \left[\frac{(2-l)V_{Srl}(R_0)}{l(l+1)} - V_{S\theta l}(R_0) \right] - (2l-1)R_0^{2l+1}\left(\frac{C_{2l0}}{l+1} - C_{5l0} \right) + (2l+1)R_0^{2l+3}C_{6l0} \right\}. \tag{E13}$$

A comment should be made. The functions $C_{1l}(r)$–$C_{6l}(r)$ are calculated by Eqs. (B13), (B14), and (C20)–(C23). If these equations are applied as they are, we get the total Eulerian streaming. If it is necessary to eliminate the Eulerian streaming that arises in the driving wave when the particle is absent, $\alpha_l(r)$ and $E_l(r)$ in Eqs. (B13), (B14), and (C20)–(C23) should be replaced by $\alpha_l(r) - \alpha_l^{(\text{ac})}(r)$ and $E_l(r) - E_l^{(\text{ac})}(r)$.

APPENDIX F: CALCULATION OF THE STOKES DRIFT VELOCITY

The Stokes drift velocity is defined by [26]

$$\boldsymbol{V}_S = \left\langle \left(\int \boldsymbol{v}^{(1)}dt \cdot \boldsymbol{\nabla} \right) \boldsymbol{v}^{(1)} \right\rangle = \frac{1}{2\omega}\text{Re}\{i\boldsymbol{v}^{(1)} \cdot \boldsymbol{\nabla}\boldsymbol{v}^{(1)*}\}. \tag{F1}$$

From Eq. (F1), one obtains

$$V_{Sr} = \frac{1}{2\omega}\text{Re}\left\{ iv_r^{(1)}\frac{\partial v_r^{(1)*}}{\partial r} + \frac{iv_\theta^{(1)}}{r}\frac{\partial v_r^{(1)*}}{\partial \theta} \right\}, \tag{F2}$$

$$V_{S\theta} = \frac{1}{2\omega}\text{Re}\left\{ iv_r^{(1)}\frac{\partial v_\theta^{(1)*}}{\partial r} + \frac{iv_r^{(1)*}v_\theta^{(1)}}{r} + \frac{iv_\theta^{(1)}}{r}\frac{\partial v_\theta^{(1)*}}{\partial \theta} \right\}. \tag{F3}$$

Substitution of Eqs. (33) and (34) into Eqs. (F2) and (F3) yields

$$V_{Sr}(r,\theta) = \frac{1}{2\omega}\text{Re}\left\{ i\sum_{n,m=0}^{\infty} V_{rn}(r)V_{rm}'^*(r)P_n(\mu)P_m(\mu) + i\sum_{n,m=1}^{\infty} \frac{V_{\theta n}(r)V_{rm}^*(r)}{r}\frac{m(m+1)}{2m+1} \right.$$
$$\left. \times \sum_{k=1}^{[(n+1)/2]} (2n-4k+3)[P_{m-1}(\mu)P_{n-2k+1}(\mu) - P_{m+1}(\mu)P_{n-2k+1}(\mu)] \right\}, \tag{F4}$$

$$V_{S\theta}(r,\theta) = \frac{1}{2\omega}\text{Re}\left(i\sum_{\substack{n=0\\m=1}}^{\infty} \left\{ V_{rn}(r)V_{\theta m}'^*(r) + \frac{V_{\theta m}(r)[V_{rn}^*(r) - n^2 V_{\theta n}^*(r)]}{r} \right\} P_n(\mu)P_m^1(\mu) \right.$$
$$\left. + i\sum_{n,m=1}^{\infty} \frac{V_{\theta m}(r)V_{\theta n}^*(r)}{r}\sum_{k=1}^{[n/2]} (2n-4k+1)P_{n-2k}(\mu)P_m^1(\mu) \right). \tag{F5}$$

Equations (F4) and (F5) are expanded as follows:

$$V_{Sr}(r,\theta) = \sum_{l=0}^{\infty} V_{Srl}(r)P_l(\mu), \tag{F6}$$

$$V_{S\theta}(r,\theta) = \sum_{l=1}^{\infty} V_{S\theta l}(r)P_l^1(\mu). \tag{F7}$$

Calculation of the expansion coefficients, with the use of Eqs. (G11)–(G13), (G15), and (G16), yields

$$V_{Srl}(r) = \frac{2l+1}{2\omega}\text{Re}\left\{ i\sum_{n=0}^{\infty} V_{rn}(r)\sum_{m=|l-n|}^{l+n} \frac{(C_{l0n0}^{m0})^2}{2m+1}V_{rm}'^*(r) + i\sum_{n=1}^{\infty}\sum_{m=1}^{[(n+1)/2]} (2n-4m+3)\frac{V_{\theta n}(r)}{r} \right.$$
$$\left. \times \sum_{k=|l-(n-2m+1)|}^{l+n-2m+1} \frac{(C_{l0(n-2m+1)0}^{k0})^2}{2k+1}\left[\frac{(k+1)(k+2)}{2k+3}V_{r(k+1)}^*(r) - \frac{k(k-1)}{2k-1}V_{r(k-1)}^*(r) \right] \right\}, \tag{F8}$$

$$V_{S\theta l}(r) = \frac{2l+1}{2\omega\sqrt{l(l+1)}}\mathrm{Re}\left(i\sum_{n=0}^{\infty}\sum_{\substack{m=|n-l| \\ m\geqslant 1}}^{n+l} \frac{\sqrt{m(m+1)}C_{n0l0}^{m0}C_{n0l1}^{m1}}{2m+1}\left\{ V_{rn}(r)V_{\theta m}'^*(r) + \frac{V_{\theta m}(r)[V_{rn}^*(r) - n^2 V_{\theta n}^*(r)]}{r}\right\}\right.$$

$$\left. + i\sum_{n=2}^{\infty}\frac{V_{\theta n}^*(r)}{r}\sum_{m=1}^{[n/2]}(2n-4m+1)\sum_{\substack{k=|n-2m-l| \\ k\geqslant 1}}^{n-2m+l} \frac{\sqrt{k(k+1)}C_{(n-2m)0l0}^{k0}C_{(n-2m)0l1}^{k1}}{2k+1}V_{\theta k}(r)\right). \tag{F9}$$

Equations (F6) and (F7) contain a part that is produced in the driving wave when the particle is absent. If it is necessary to eliminate this part, $V_{Srl}(r)$ and $V_{S\theta l}(r)$ should be replaced by $V_{Srl}(r) - V_{Srl}^{(\mathrm{ac})}(r)$ and $V_{S\theta l}(r) - V_{S\theta l}^{(\mathrm{ac})}(r)$, where $V_{Srl}^{(\mathrm{ac})}$ and $V_{S\theta l}^{(\mathrm{ac})}(r)$ are calculated by Eqs. (F8) and (F9) using the expressions for $V_{rn}(r)$ and $V_{\theta n}(r)$ from Eq. (E8).

APPENDIX G: MATHEMATICAL FORMULAS USED IN CALCULATIONS

Here, auxiliary mathematical formulas are provided that are used in the principal calculations. In the equations that follow, the prime denotes the derivative with respect to an argument in brackets, $[\cdots]$ in the upper bounds of sums means the integer part of an expression in brackets, $C_{l_1 m_1 l_2 m_2}^{LM}$ are the Clebsch-Gordan coefficients, and δ_{nm} is the Kronecker delta.

We use the following formulas for $P_n(\mu)$ and $P_n^1(\mu)$ [44]:

$$P_n^1(\mu) = -\sqrt{1-\mu^2}P_n'(\mu), \tag{G1}$$

$$\sqrt{1-\mu^2}P_n^{1'}(\mu) + \mu P_n'(\mu) = n(n+1)P_n(\mu), \tag{G2}$$

$$(1-\mu^2)P_n'(\mu) = \frac{n(n+1)}{2n+1}[P_{n-1}(\mu) - P_{n+1}(\mu)], \tag{G3}$$

$$P_n'(\mu) = \sum_{k=1}^{[(n+1)/2]}(2n-4k+3)P_{n-2k+1}(\mu), \quad n \geqslant 1, \tag{G4}$$

$$\mu P_n'(\mu) = nP_n(\mu) + P_{n-1}'(\mu), \tag{G5}$$

$$(1-\mu^2)P_n^{1''}(\mu) - 2\mu P_n^{1'}(\mu) = \left[\frac{1}{1-\mu^2} - n(n+1)\right]P_n^1(\mu). \tag{G6}$$

With the help of these formulas, the following identities are derived:

$$\frac{1}{\sin\theta}\frac{d}{d\theta}\left[\sin\theta P_n(\mu)P_m^1(\mu)\right] = -m(m+1)P_n(\mu)P_m(\mu) + \frac{m(m+1)}{2m+1}\sum_{k=1}^{[(n+1)/2]}(2n-4k+3)[P_{m-1}(\mu)P_{n-2k+1}(\mu)$$

$$- P_{m+1}(\mu)P_{n-2k+1}(\mu)], \tag{G7}$$

$$P_n^1(\mu)P_m^1(\mu) = \frac{m(m+1)}{2m+1}\sum_{k=1}^{[(n+1)/2]}(2n-4k+3)[P_{m-1}(\mu)P_{n-2k+1}(\mu) - P_{m+1}(\mu)P_{n-2k+1}(\mu)], \tag{G8}$$

$$\sqrt{1-\mu^2}P_n^{1'}(\mu)P_m^1(\mu) = \left[n^2 P_n(\mu) - \sum_{k=1}^{[n/2]}(2n-4k+1)P_{n-2k}(\mu)\right]P_m^1(\mu), \tag{G9}$$

$$(1-\mu^2)\left[P_n^1(\mu)P_m^{1''}(\mu) - 2P_n^{1'}(\mu)P_m^{1'}(\mu)\right] - \mu P_n^1(\mu)P_m^{1'}(\mu)$$

$$= nm[1 - m(2n+1)]P_n(\mu)P_m(\mu) - m(m+1)P_n^1(\mu)P_m^1(\mu) + 2n(n+1)\sum_{k=1}^{[m2]}(2m-4k+1)P_n(\mu)P_{m-2k}(\mu)$$

$$+ m(m+1)\sum_{k=1}^{[n/2]}(2n-4k+1)P_{n-2k}(\mu)P_m(\mu)$$

$$+ \frac{n(n+1)}{2n+1}[P_{n-1}(\mu) - P_{n+1}(\mu)]\sum_{k=1}^{[(m+1)/2]}(2m-4k+3)P_{m-2k+1}(\mu), \tag{G10}$$

$$\mu P_n(\mu)P_m'(\mu) = mP_n(\mu)P_m(\mu) + \sum_{k=1}^{[m/2]}(2m-4k+1)P_{m-2k}(\mu)P_n(\mu), \tag{G11}$$

$$\mu P_n^1(\mu)P_m^{1'}(\mu) = -nm^2 P_n(\mu)P_m(\mu) + \sum_{k=1}^{[m/2]} n(2m-4k+1)P_{m-2k}(\mu)P_n(\mu) - \sum_{k=1}^{[n/2]} m^2(2n-4k+1)P_{n-2k}(\mu)P_m(\mu)$$

$$+ \sum_{k=1}^{[n/2]}\sum_{s=1}^{[m/2]}(2n-4k+1)(2m-4s+1)P_{n-2k}(\mu)P_{m-2s}(\mu), \tag{G12}$$

$$P_n'(\mu)P_m'(\mu) = \sum_{k=1}^{[(n+1)/2]}\sum_{s=1}^{[(m+1)/2]}(2n-4k+3)(2m-4s+3)P_{n-2k+1}(\mu)P_{m-2s+1}(\mu), \tag{G13}$$

$$\mu^2 P_n'(\mu)P_m'(\mu) = nmP_n(\mu)P_m(\mu) + \sum_{k=1}^{[m/2]} n(2m-4k+1)P_{m-2k}(\mu)P_n(\mu)$$

$$+ \sum_{k=1}^{[n/2]} m(2n-4k+1)P_{n-2k}(\mu)P_m(\mu) + \sum_{k=1}^{[n/2]}\sum_{s=1}^{[m/2]}(2n-4k+1)(2m-4s+1)P_{n-2k}(\mu)P_{m-2s}(\mu). \tag{G14}$$

To calculate integrals with products of $P_n(\mu)$ and $P_n^1(\mu)$, we use the following identity:

$$P_{l_1}^{m_1}(\mu)P_{l_2}^{m_2}(\mu) = \sqrt{\frac{(l_1+m_1)!(l_2+m_2)!}{(l_1-m_1)!(l_2-m_2)!}}\sum_{l=|l_1-l_2|}^{l_1+l_2}\sqrt{\frac{(l-m_1-m_2)!}{(l+m_1+m_2)!}}C_{l_10l_20}^{l0}C_{l_1m_1l_2m_2}^{l(m_1+m_2)}P_l^{m_1+m_2}(\mu). \tag{G15}$$

This identity follows from Eq. (9) of Sec. 5.6 of Ref. [39].
Making use of Eq. (G15) along with the orthogonality condition for $P_n(\mu)$,

$$\int_{-1}^{1}P_n(\mu)P_m(\mu)d\mu = \frac{2}{2n+1}\delta_{nm}, \tag{G16}$$

one obtains the following integrals:

$$\int_{-1}^{1}P_l(\mu)P_n(\mu)P_m(\mu)d\mu = \sum_{m=|l-n|}^{l+n}\frac{2}{2m+1}\left(C_{l0n0}^{m0}\right)^2, \tag{G17}$$

$$\int_{-1}^{1}P_l(\mu)P_{m-1}(\mu)P_{n-2k+1}(\mu)d\mu = \sum_{m-1=|l-(n-2k+1)|}^{l+n-2k+1}\frac{2}{2m-1}\left(C_{l0(n-2k+1)0}^{(m-1)0}\right)^2, \tag{G18}$$

$$\int_{-1}^{1}P_l(\mu)P_{m+1}(\mu)P_{n-2k+1}(\mu)d\mu = \sum_{m+1=|l-(n-2k+1)|}^{l+n-2k+1}\frac{2}{2m+3}\left(C_{l0(n-2k+1)0}^{(m+1)0}\right)^2, \tag{G19}$$

$$\int_{-1}^{1}P_l(\mu)P_{n-2k}(\mu)P_{m-2s}(\mu)d\mu = \sum_{q=|l-(n-2k)|}^{l+n-2k}\left(C_{l0(n-2k)0}^{q0}\right)^2\frac{2}{2q+1}\delta_{q(m-2s)}. \tag{G20}$$

From Eq. (G15) and the orthogonality condition for $P_n^1(\mu)$,

$$\int_{-1}^{1}P_n^1(\mu)P_m^1(\mu)d\mu = \frac{2n(n+1)}{2n+1}\delta_{nm}, \tag{G21}$$

one obtains

$$\int_{-1}^{1}P_n(\mu)P_m^1(\mu)P_l^1(\mu)d\mu = 2\sqrt{l(l+1)}\sum_{\substack{m=|n-l|\\m\geqslant 1}}^{n+l}\frac{\sqrt{m(m+1)}C_{n0l0}^{m0}C_{n0l1}^{m1}}{2m+1}, \tag{G22}$$

$$\int_{-1}^{1}P_{n-2k}(\mu)P_m^1(\mu)P_l^1(\mu)d\mu = 2\sqrt{l(l+1)}\sum_{\substack{m=|n-2k-l|\\m\geqslant 1}}^{n-2k+l}\frac{\sqrt{m(m+1)}C_{(n-2k)0l0}^{m0}C_{(n-2k)0l1}^{m1}}{2m+1}. \tag{G23}$$

[1] M. Oliveira, M. A. Alves, and F. T. Pinho, Microfluidic flows in viscoelastic fluids, in *Mixing in Laminar Fluid Flows. Reviews of Nonlinear Dynamics and Complexity*, edited by R. Grigoriev (Wiley-Blackwell, Berlin, 2011), Chap. 6, pp. 131–165.

[2] G. D'Avino, F. Greco, and P. L. Maffettone, Particle migration due to viscoelasticity of the suspending liquid and its relevance in microfluidic devices, Annu. Rev. Fluid Mech. **49**, 341 (2017).

[3] Y. Zhou, Z. Ma, and Y. Ai, Submicron particle concentration and patterning with ultralow frequency acoustic vibration, Anal. Chem. **92**, 12795 (2020).

[4] A. M. Leshansky, A. Bransky, N. Korin, and U. Dinnar, Tunable Nonlinear Viscoelastic Focusing in a Microfluidic Device, Phys. Rev. Lett. **98**, 234501 (2007).

[5] J. Zhou and I. Papautsky, Viscoelastic microfluidics: Progress and challenges, Microsyst. Nanoeng. **6**, 113 (2020).

[6] W. L. Nyborg, Acoustic streaming, in *Physical Acoustics*, edited by W. P. Mason (Academic, New York, 1965), Vol. IIB, pp. 266–331.

[7] J. Lighthill, Acoustic streaming, J. Sound Vib. **61**, 391 (1978).

[8] N. Riley, Acoustic streaming, in *Encyclopedia of Acoustics*, edited by M. J. Crocker (Wiley, New York, 1997), pp. 321–327.

[9] W. L. Nyborg, Acoustic streaming, in *Nonlinear Acoustics*, edited by M. F. Hamilton and D. T. Blackstock (Academic, San Diego, CA, 1998), pp. 207–231.

[10] N. Riley, Steady streaming, Annu. Rev. Fluid Mech. **33**, 43 (2001).

[11] S. Boluriaan and P. J. Morris, Acoustic streaming: From Rayleigh to today, Int. J. Aeroacoust. **2**, 255 (2003).

[12] M. Wiklund, R. Green, and M. Ohlin, Acoustofluidics 14: Applications of acoustic streaming in microfluidic devices, Lab Chip **12**, 2438 (2012).

[13] A. A. Doinikov, J. Fankhauser, and J. Dual, Nonlinear dynamics of a solid particle in an acoustically excited viscoelastic fluid. II. Acoustic radiation force, Phys. Rev. E **104**, 065108 (2021).

[14] L. D. Landau and E. M. Lifshitz, *Theory of Elasticity* (Pergamon Press, Oxford, 1970).

[15] L. D. Landau and E. M. Lifshitz, *Fluid Mechanics* (Pergamon Press, Oxford, 1987).

[16] A. Morozov and S. E. Spagnolie, Introduction to complex fluids, in *Complex Fluids in Biological Systems*, edited by S. E. Spagnolie (Springer, New York, 2015), pp. 3–52.

[17] D. D. Joseph, *Fluid Dynamics of Viscoelastic Liquids* (Springer-Verlag, New York, 1990).

[18] J. Ortín, Stokes layers in oscillatory flows of viscoelastic fluids, Philos. Trans. R. Soc., A **378**, 20190521 (2019).

[19] R. B. Bird, R. C. Armstrong, and O. Hassager, *Dynamics of Polymeric Liquids* (Wiley, New York, 1987).

[20] A. Ponce-Torres, A. J. Acero, M. A. Herrada, and J. M. Montanero, On the validity of the Jeffreys (Oldroyd-B) model to describe the oscillations of a viscoelastic pendant drop, J. Non-Newtonian Fluid Mech. **260**, 69 (2018).

[21] A. Shima, T. Tsujino, and H. Nanjo, Nonlinear oscillations of gas bubbles in viscoelastic fluids, Ultrasonics **24**, 142 (1986).

[22] J. S. Allen and R. A. Roy, Dynamics of gas bubbles in viscoelastic fluids. I. linear viscoelasticity, J. Acoust. Soc. Am. **107**, 3167 (2000).

[23] M. A. Hintermüller, E. Reichel, and B. Jakoby, Modeling of acoustic streaming in viscoelastic fluids, in *2017 IEEE Sensors* (IEEE, New York, 2017).

[24] K. Cahill, *Physical Mathematics* (Cambridge University Press, Cambridge, 2013).

[25] C. Eckart, Vortices and streams caused by sound waves, Phys. Rev. **73**, 68 (1948).

[26] M. S. Longuet-Higgins, Viscous streaming from an oscillating spherical bubble, Proc. R. Soc. London, Ser. A **454**, 725 (1998).

[27] G. Wypych, *Handbook of Polymers* (ChemTec Publishing, Toronto, 2016).

[28] F. E. Bailey and R. W. Callard, Some properties of poly (ethy1ene oxide)[1] in aqueous solution, J. Appl. Polym. Sci. **1**, 56 (1959).

[29] D. M. Yu, G. L. Amidon, N. D. Weiner, and A. H. Goldberg, Viscoelastic properties of poly(ethylene oxide) solution, J. Pharm. Sci. **83**, 1443 (1994).

[30] P. Gonzalez-Tello, F. Camacho, and G. Blazquez, Density and viscosity of concentrated aqueous solutions of polyethylene glycol, J. Chem. Eng. Data **39**, 611 (1994).

[31] K. W. Ebagninin, A. Benchabane, and K. Bekkour, Rheological characterization of poly (ethylene oxide) solutions of different molecular weights, J. Colloid Interface Sci. **336**, 360 (2009).

[32] R. Joshi and N. D. Kandpal, Viscometric properties of aqueous solutions of poly (ethylene) glycols at 15 °C, Der Pharmacia Lettre **7**, 126 (2015).

[33] F. Tian, W. Zhang, L. Cai, S. Li, G. Hu, Y. Cong, C. Liu, T. Li, and J. Sun, Microfluidic co-flow of Newtonian and viscoelastic fluids for high-resolution separation of microparticles, Lab Chip **17**, 3078 (2017).

[34] H. G. Kye, B. S. Park, J. M. Lee, M. G. Song, H. G. Song, C. D. Ahrberg, and B. G. Chung, Dual-neodymium magnet-based microfluidic separation device, Sci. Rep. **9**, 9502 (2019).

[35] J. B. Bostwick and P. H. Steen, Dynamics of sessile drops. Part 1. Inviscid theory, J. Fluid Mech. **760**, 5 (2014).

[36] C.-T. Chang, J. B. Bostwick, S. Daniel, and P. H. Steen, Dynamics of sessile drops. Part 2. Experiment, J. Fluid Mech. **768**, 442 (2015).

[37] S. Cleve, M. Guédra, C. Mauger, C. Inserra, and P. Blanc-Benon, Microstreaming induced by acoustically trapped, non-spherically oscillating microbubbles, J. Fluid Mech. **875**, 597 (2019).

[38] G. Regnault, C. Mauger, P. Blanc-Benon, A. A. Doinikov, and C. Inserra, Signatures of microstreaming patterns induced by non-spherically oscillating bubbles, J. Acoust. Soc. Am. **150**, 1188 (2021).

[39] D. A. Varshalovich, A. N. Moskalev, and V. K. Khersonskii, *Quantum Theory of Angular Momentum* (World Scientific, Singapore, 1988).

[40] D. Zwillinger, *Standard Mathematical Tables and Formulae* (CRC, Boca Raton, FL, 2003).

[41] W. E. Boyce and R. C. DiPrima, *Elementary Differential Equations and Boundary Value Problems* (Wiley, New York, 2001).

[42] L. I. Sedov, *Mechanics of Continuous Media* (World Scientific, Singapore, 1997), Vol. 1.

[43] L. G. Loitsyanskii, *Mechanics of Liquids and Gases* (Pergamon Press, Oxford, 1966).

[44] M. Abramowitz and I. A. Stegun, *Handbook of Mathematical Functions with Formulas, Graphs and Mathematical Tables* (Dover, New York, 1972).